Journal of the Brazilian Society of Mechanical Sciences and Engineering (2026) 48:1030
https://doi.org/10.1007/s40430-026-07029-7

TECHNICAL PAPER

Synergistic performance of vortex cooling and surfactant-modified CuO nanolubrication when clean milling of Inconel X-750

Cemal Şimşek[1] · Çağrı Vakkas Yıldırım[2,3] · Şenol Şirin[4]

Received: 9 June 2026 / Accepted: 30 September 2026
© The Author(s), under exclusive licence to The Brazilian Society of Mechanical Sciences and Engineering 2026

Abstract

The sustainable clean machining of nickel-based superalloys, specifically Inconel X-750, is traditionally constrained by rapid tool degradation and severe thermal accumulation. To address a critical research gap in eco-benign thermal management for difficult-to-cut superalloys, this study presents a novel hybrid cooling/lubrication framework that integrates vortex tube cryogenic cooling with Minimum Quantity Lubrication (MQL) using CuO nanofluids. The primary novelty lies in systematically establishing the synergistic coupling between sub-zero convective cooling and surfactant-functionalized nano-tribological behavior, evaluated through three distinct charge-state surfactants: PVP (non-ionic), SDS (anionic), and CTAB (cationic). Experimental results revealed that the hybrid vortex-assisted nanofluid system drastically transformed the thermomechanical interactions at the tool-chip interface. In particular, PVP-modified nanofluids combined with vortex cooling demonstrated superior overall performance, achieving the highest cooling capacity by reducing the cutting temperature by up to 37.77% compared to dry milling, while simultaneously improving surface quality by reducing the average roughness (Ra) by 64.04%. Furthermore, the combined anti-friction tribofilm and enhanced heat dissipation suppressed adhesive and abrasive tool wear, extending tool life by 58.36%. Beyond empirical performance gains, the key scientific contribution of this work is elucidating the mechanistic role of surfactant electrostatic/steric stabilization on droplet wettability, interfacial film formation, and wear suppression during superalloy milling. These insights provide a scalable, ecologically viable paradigm for the high-integrity precision manufacturing of critical aerospace components.

Technical Editor: Lincoln Cardoso Brandao.

✉ Çağrı Vakkas Yıldırım
cvyildirim@erciyes.edu.tr

[1] Graduate School of Natural and Applied Sciences, Department of Aeronautical and Astronautical Engineering, Erciyes University, Kayseri, Turkey

[2] Department of Airframes and Powerplants, Erciyes University, Kayseri, Turkey

[3] Aviation Studies Application and Research Center, Erciyes University, Kayseri, Turkey

[4] Department of Mechatronics Engineering, Düzce University, Düzce, Turkey

Published online: 13 November 2026

Graphical abstract

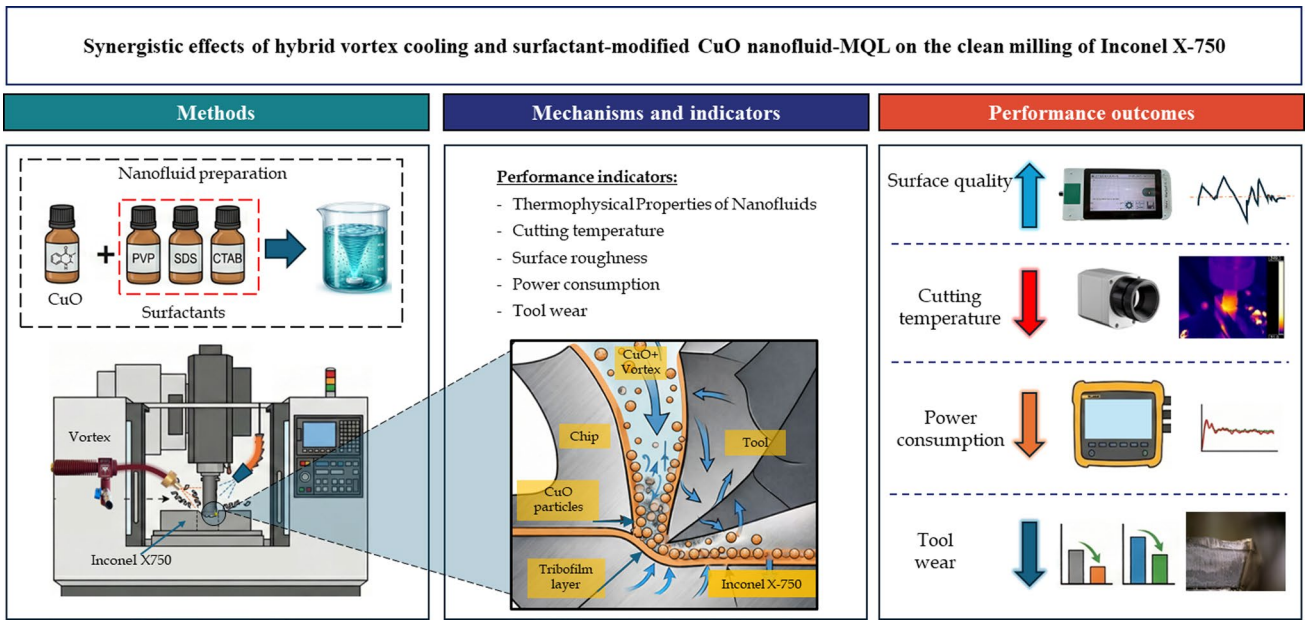

Highlights

- Vortex-assisted MQL with surfactant-modified CuO nanofluids was investigated.
- Surfactant addition (PVP, SDS, and CTAB) to CuO nanofluids enhanced cooling capability.
- The hybrid cooling strategy significantly reduced tool wear and cutting temperature.
- Surface quality of machined Inconel X-750 was substantially improved.
- Proposed method offers a sustainable alternative to conventional cutting fluids.

Keywords Hybrid cooling/lubrication · Clean milling · Surfactant modification · Vortex tube cooling · CuO nanofluid · Inconel X-750

1 Introduction

Nickel-based superalloys are widely used in applications requiring high temperatures and harsh operating conditions, such as power generation and industrial gas turbines [1], as well as rocket and high-temperature propulsion applications [2]. Additionally, these superalloys are highly preferred materials in the chemical industry, for the manufacture of equipment requiring corrosion resistance, for systems operating in high-stress underground environments in the oil and gas sector, for nuclear power plants, and for many critical industries such as maritime. In addition, high-pressure turbine blades, disks, combustion chamber components, nozzle guide vane (NGV) components, combustion chamber walls, and exhaust systems are among the many components in the "hot zone" of jet engines in aircraft that are subjected to high temperatures that are made from nickel-based superalloys [3]. The primary causes of these materials' broad appeal are their mechanical properties, thermal stability, and resistance to oxidation and corrosion at elevated temperatures. The fine, regularly distributed γ′ precipitates in its structure hinder dislocation movement, limiting flow and creep even at high temperatures through partial transition and bypass mechanisms [4]. Additionally, the dissolution of heavy elements such as Mo, W, Re, and Ta in the Ni matrix hinders dislocation motion. This results in high strength [5]. Moreover, these elements also support thermal stability. Thus, they can remain stable even at high temperatures [4]. In terms of corrosion resistance, the Cr and Al elements in the alloy form a tight, adhesive, low-diffusion chromium and/or alumina layer on the surface of the material at high temperatures. Thus, oxygen penetration is prevented, thereby preventing oxidation that may occur in the material [6]. However, the high-temperature resistance, low thermal conductivity, strength, corrosion/oxidation resistance, and rapid work hardening that occur during processing are among the material's fundamental properties, making it difficult to cut. The ductile behavior of the material increases cutting forces during chip removal, making chip breakage difficult and leading to vibration [7, 8]. Additionally, the tendency

of the material to undergo chemical reactions complicates machining [9]. Cutting fluid is recommended as an auxiliary during the processing of nickel-based superalloys due to these factors.

The use of cutting fluid during chip removal can alleviate both mechanical and thermal issues. Cutting fluid can be used to regulate cutting temperature, particularly in heavy machining, when hard-to-machine materials are processed quickly [10]. Additionally, cutting fluids improve surface quality, lower cutting temperatures by reducing friction, eliminate chips from the cutting zone, and prolong tool life [11–13]. However, conventional cutting fluids have some disadvantages. For example, the supply, maintenance, filtration, and disposal costs of cutting fluids can increase total production costs [14]. Mineral-based cutting fluids, in particular, pose risks to the environment and worker health [15]. Schwarz et al. [16] claimed that exposure to classical cutting fluids via aerosols is a significant problem, that these aerosols are respirable (1–10 μm), and that inhalation can cause respiratory problems such as asthma, chronic bronchitis, and hypersensitivity pneumonitis. In another study, Wickramasinghe et al. [17] stated that mineral-based cutting fluids can cause cancer, skin irritation, and respiratory problems. In another study, Calvert et al. [18] claimed that workers exposed to metalworking fluids had an increased risk of laryngeal, pancreatic, skin, and bladder cancer. From an environmental perspective, Cheng et al. [19] emphasized that used metalworking fluids contain complex organic compounds, biocides, and other pollutants, and therefore cause both water and soil pollution when released into the environment. In addition, if parameters such as nozzle placement and cutting fluid pressure are not optimized, they may be insufficient for cooling and lubrication [20]. For this reason, many industrial organizations and researchers today continue to work on both alternative methods and the parameter optimization of existing methods. While research continues on various cooling and lubrication methods, MQL, nanofluids, vortex cooling, and hybrid approaches that combine these techniques are gaining prominence. The MQL system delivers an oil-based lubricant to the cutting surface by atomizing it with compressed air at a low flow rate. It is also known as small quantity lubrication or near-dry machining [21, 22]. Because it uses soluble lubricants and has very little oil, it is regarded as an environmentally beneficial cooling and lubricating approach when compared to traditional cutting fluids [13]. In their study, Wang and Liu [23] reported that using MQL reduced cutting fluid consumption by 1000 times, thereby reducing environmental pollution and complying with clean production principles. The MQL system provides relatively good lubrication cooling, especially under light- and medium-duty machining conditions [21]. However, the literature discusses that cooling properties are insufficient, especially under heavy processing conditions. Wu et al. [24] used the MQL system during the machining of hardened steel. Although the MQL system provides effective lubrication, it has been reported that the oil film fails at high temperatures and that the system is insufficient for cooling. According to research, the MQL system is unable to tolerate large heat loads, especially when cutting hard materials quickly. In another study, Patra and Swain [25] emphasized that the cooling capacity of the MQL system is limited in applications with high thermal loads. Bhowmik et al. [26] claimed that one obstacle to the widespread industrial adoption of MQL systems is their limited cooling efficiency. The use of nano-cutting fluids is the first technique that springs to mind in these situations.

In its broadest definition, nanofluids are colloidal suspensions created by scattering nanoparticles inside a base fluid. The strategy of employing micro- and nanoscale additives or fillers to tailor thermomechanical and tribological properties is a widely accepted approach in advanced materials engineering. For instance, recent fundamental studies have demonstrated that integrating solid fillers, such as Silicon Carbide (SiC) or Carbon Nanotubes (CNTs), into composite matrices significantly enhances thermal stability, friction resistance, and overall structural integrity under demanding manufacturing conditions [27, 28]. A similar mechanistic principle applies to metal cutting: when metal oxide nanoparticles (e.g., CuO) are dispersed in a base fluid, they serve as mobile fillers. During the machining process, these nano-fillers penetrate the tool-chip interface, improving local heat dissipation and forming a protective, solid-lubricant-like tribofilm layer that substantially reduces tool wear. In nanofluids, the particles are typically selected from metals (Cu, Ag, etc.), metal oxides (Al_2O_3, TiO_2, etc.), carbides, or carbon-based materials (graphite, graphene, carbon nanotubes, etc.), while the base fluid is usually water, ethylene, glycol, mineral oil, vegetable oil, etc. [29]. The primary justification for selecting these fluids is because they have better thermophysical characteristics than base cutting fluids, including viscosity, heat transfer coefficient, thermal conductivity, and lubricity [30]. In nanofluid use, a very small amount (at the ml/h level) is sprayed onto the nanofluid cutting zone to form a thin film. The nanoparticles in the nanofluid enhance thermal conductivity to varying degrees depending on particle type, thereby providing thermal control and altering tribological behavior at contact surfaces through the third-body (rolling/solid-film) effect [31]. This can significantly increase machining efficiency. According to Korkmaz and Gupta [32], the addition of nanoparticles can enhance the thermal characteristics of base fluids, including density, viscosity, and thermal conductivity, hence boosting heat transfer capacity. The use of dispersed nanoparticles to significantly enhance the thermal

conductivity and heat-dissipation capacity of base fluids is an established thermodynamic principle in various engineering fields. For instance, recent comprehensive studies have demonstrated that (hybrid) nanofluids play a critical role in enhancing effective cooling, thermal performance, and energy storage in advanced thermal systems, such as solar air heaters [33]. Drawing on this universal mechanism of high-efficiency thermal management, the present study employs surfactant-modified CuO nanofluids to optimize localized heat generation during the machining of Inconel X-750. Analogous to macroscopic thermal systems, the nanoparticles within the cutting fluid act as ultra-efficient heat carriers, helping to significantly reduce cutting temperatures at the tool-chip-workpiece interface. Fernando et al. [34] reported that nanoparticles settle at the workpiece-cutting tool interface, exhibiting rolling, layering, and film-forming effects, thereby reducing friction and increasing machining efficiency. In another study, Hu et al. [35] reported that nanoparticles can penetrate the cutting/workpiece interface to form a "protective layer" (tribofilm) that can reduce friction forces. This reduction in friction increases machining efficiency. As noted in the literature review, nanofluids are among the cooling methods that increase machining efficiency and, in this respect, serve as alternatives to conventional cutting fluids. However, there are some disadvantages to using nanofluids. One of the most well-known disadvantages is the issue of stability. The dispersion stability of nanoparticles is generally difficult to achieve and can lead to aggregation [36–39]. The most common and effective method for minimizing this problem is the use of surfactants. [40]. Surfactants are molecules with hydrophilic and hydrophobic ends. They adsorb onto the surfaces of particles in the nanofluid, creating electrostatic or steric barriers between particles. These barriers balance van der Waals attractive forces and reduce the tendency for agglomeration [41]. In other words, with the use of surfactants, the particles are held in equilibrium by repulsive forces rather than approaching each other, thereby increasing colloidal stability [41]. Additionally, prior research has shown that the application of surfactants improves tribological performance, atomization and spraying behavior, colloidal stability, and processing efficiency [22, 42]. However, the effect of surfactant use in chip-removal operations depends on the surfactant type, concentration, nanoparticle type, base fluid, and process conditions. Therefore, it is important to test different parameters and combinations. Another problem encountered with nanofluids is insufficient cooling performance, especially under heavy processing conditions. According to Abellán-Nebot et al. [43], agglomeration or low wettability problems arise due to excessive nano-additive addition, which negatively affects cooling performance. According to Dennison et al. [44], although nanofluids offer many advantages, they cannot fully realize their cooling potential due to stability and spray issues. Manikanta et al. [45] reported an increase in cutting temperature in their study with triple-hybrid nanoparticles. This indicates insufficient cooling performance. One of the preferred methods to increase cooling performance in such applications is the use of vortex or hybrid cooling with cutting fluids. The vortex tube is a practical cooling method that operates according to the principles of vortex flow. The vortex tube receives compressed air from the compressor. The compressed air from the compressor is separated into two streams by the vortex tube, one of which has a lower temperature than the entering air. The vortex tube can achieve a temperature drop of approximately 70 °C [46]. This system's greatest benefit is that it uses only compressed air to produce low-temperature air and has no moving parts. Thus, there is no need for electricity or freon [47]. According to some studies, processing performance is enhanced when vortices are used in chip-removal procedures [48–51]. However, studies in the literature indicate that better results are achieved when the vortex tube is used in conjunction with high-lubricity cooling systems such as MQL or nano-MQL. For example, according to Šterpin Valić et al. [52], they turned X20Cr13 martensitic stainless steel by combining an MQL system with a vortex tube, thereby improving machining efficiency. Mohd Khalil et al. [53] investigated the shape memory alloy NiTi under dry, nanoMQL, and nanoMQL+vortex conditions and reported that hybrid cooling yielded better results in terms of surface roughness, tool wear, cutting temperature, and cutting forces. Singh and Sharma [54] compared pure MQL with vortex tube + MQL during machining of commercial pure titanium grade 2. According to the researchers' analysis of experimental data, hybrid cooling significantly reduced tool wear, power consumption, cutting force, and surface quality. Similarly, Singh et al. [55] compared pure MQL with vortex-assisted MQL during the machining of commercial pure titanium grade 2. According to the experimental results, the vortex-assisted MQL system achieved higher machining efficiency across all outputs. In the hard turning of hardened AISI D3 steel, Ayhan et al. [56] examined the effects of ten distinct environmentally friendly cooling/lubrication techniques (dry, MQL, vortex, graphene nanoparticle nanofluid (GPN), graphene quantum dot nanofluid (GQDs), and their hybrid combinations) on side wear (VBmax), tool wear characterization, cutting temperature, energy consumption, and surface roughness. The researchers concluded that the Vortex + GPN/GQDs hybrid cooling approach performed the best based on the experimental data.

As noted in the literature review, each cooling and lubrication system used in chip-removal processes has distinct advantages and limitations. Moreover, the magnitude of

these effects is strictly governed by the selected machining technique, cutting parameters, and the specific configurations of the cooling methods. The highly interactive nature of these variables remains a prominent challenge in literature, emphasizing that the "clean machining" paradigm still necessitates profound mechanistic investigations rather than purely empirical observations. To address this fundamental gap, this study introduces a synergistic hybrid cooling and lubrication framework that uniquely integrates vortex tube cold air delivery with Minimum Quantity Lubrication (MQL) utilizing CuO nanofluids. The primary novelty of this research is the systematic functionalization of these nanofluids with three distinctly charged surfactants—PVP, SDS, and CTAB—to comparatively evaluate their interactive thermo-tribological behaviors under the extreme mechanical stresses of Inconel X-750 milling. Moving beyond a conventional broad experimental design, the core scientific contribution of this manuscript lies in elucidating how the electrostatic and steric properties of varying surfactants dictate nanoparticle wettability, localized heat dissipation, and the precise formation mechanisms of protective tribofilm at the tool-chip interface. This comprehensive approach aims not only to make significant contributions to existing literature but also to serve as a valuable reference source for researchers and manufacturers conducting similar studies in the future. Despite recent advancements in MQL and cryogenic cooling, there remains a significant research gap regarding the synergistic use of sub-zero vortex cooling and nanofluids modified with specific surfactants—particularly for the machining of difficult-to-cut superalloys (i.e., Inconel X-750) under demanding conditions. To address this gap, this study proposes a highly innovative and eco-friendly hybrid machining approach. The core innovation of the research lies in the systematic investigation of the phenomenological and thermomechanical synergy between localized cryogenic vortex and CuO nanofluids modified with surfactants representing three different charge states: non-ionic PVP, anionic SDS, and cationic CTAB. Ultimately, the proposed hybrid strategy yields highly efficient, sustainable, and clean industrial applications that directly meet the rigorous high-precision manufacturing requirements of the aerospace and advanced metalworking sectors.

2 Experimental materials and methods

2.1 Material, cutting tool, and machine center

In this study, a precipitation-hardened nickel-based superalloy material, Inconel X-750, commonly used in the aerospace and nuclear industries, with dimensions of 150 × 100 × 17.3 mm, was used. The alloy exhibits superior properties such as high corrosion resistance, excellent resistance to corrosive environments, and high fatigue and creep strength even at temperatures above 700 °C [57]. The dimensions, properties, and chemical composition of the Inconel X-750 superalloy material are provided in Fig. 1.

The superalloy material was prepared for machining experiments by being rigidly clamped to an 11-kW Delta Seiki vertical machining center. During the preparation phase, the clamp, workpiece, and machine table were checked for perpendicularity and parallelism using a comparator. Sandvik CoroMill® 490 inserts, designed for milling, were used in the experimental work. The cutting tool had 4 different cutting edges: ISO code 490R-08T308E, chip-breaker type ML, grade S30T, and PVD TiAlN coating. In each experiment, a new cutting edge was used, coded in machinability tests, and stored in separate boxes for different measurements (SEM, wear, control). The 490-025A20-08L holder was used to firmly mount the cutting tools to the machine.

The purpose of the experimental investigation was to ascertain how cooling and lubrication conditions affected the long-term forming of Inconel X-750 superalloy material. This was accomplished by maintaining consistent cutting speed, feed rate, axial depth, and radial depth throughout the trial. Preliminary trials, the manufacturer's catalog, and literature were used to determine the cutting settings. The cutting speed, feed rate, axial depth, and radial depth were maintained at 70 m/min, 0.2 mm/rev, 0.5 mm, and 15 mm (60 percent of the cutting tool diameter) accordingly, under all cooling and lubrication conditions.

2.2 Cooling and lubrication conditions

Managing the extreme heat and friction at the tool-chip interface during Inconel X-750 milling necessitates a robust thermal management framework. This section outlines the specific cooling and fluid delivery strategies applied throughout the experimental trials. The following subsections detail the operational setup of the vortex system and the step-by-step formulation of the CuO nanofluids, including their specific functionalization with different charge-state surfactants.

2.2.1 Vortex cooling system

A Tecus (Türkiye) TVX-15 Ranque–Hilsch vortex tube (RHVT) was utilized in this investigation to regulate the heat in the cutting zone and produce a chilly stream from the compressed air exiting the compressor (Fig. 2). The RHVT system can be described as a simple and fixed thermodynamic device with no moving parts. It only requires a compressed-air source from the compressor, and this pressurized

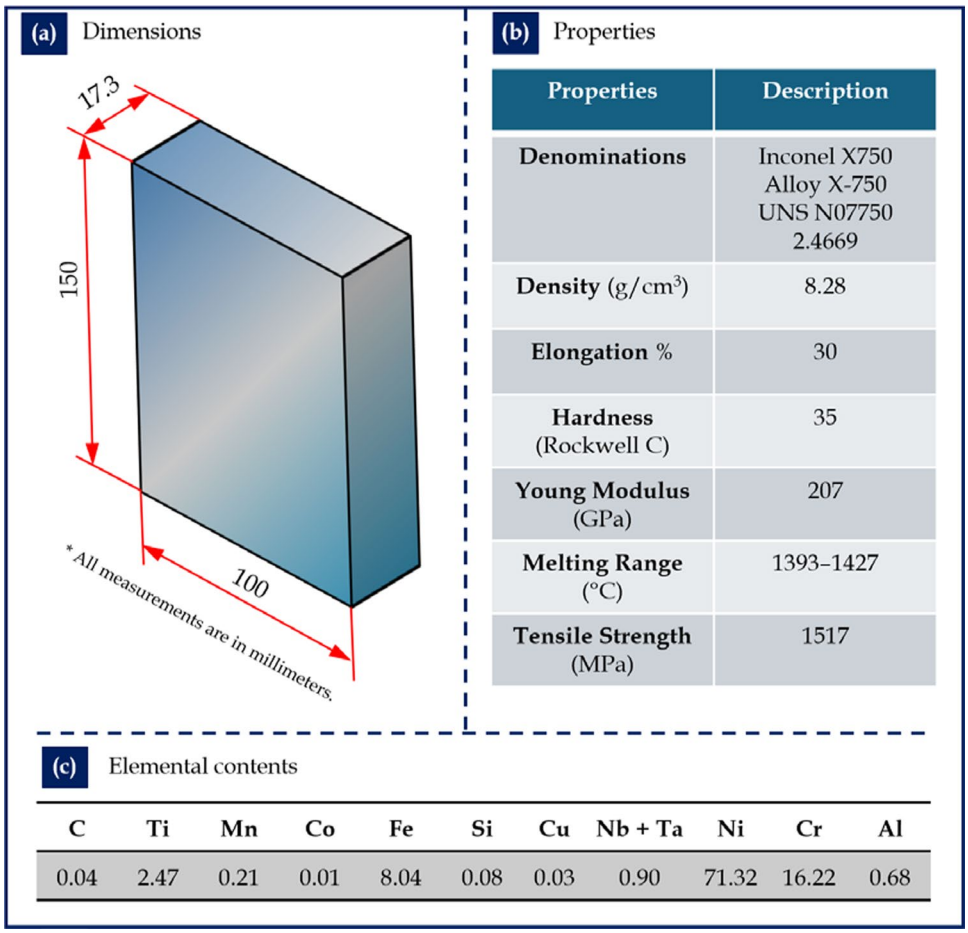

Properties	Description
Denominations	Inconel X750 Alloy X-750 UNS N07750 2.4669
Density (g/cm^3)	8.28
Elongation %	30
Hardness (Rockwell C)	35
Young Modulus (GPa)	207
Melting Range (°C)	1393–1427
Tensile Strength (MPa)	1517

C	Ti	Mn	Co	Fe	Si	Cu	Nb + Ta	Ni	Cr	Al
0.04	2.47	0.21	0.01	8.04	0.08	0.03	0.90	71.32	16.22	0.68

Fig. 1 Inconel X-750 superalloy, **a** dimensions, **b** properties, and **c** elemental contents (*source from manufacturer)

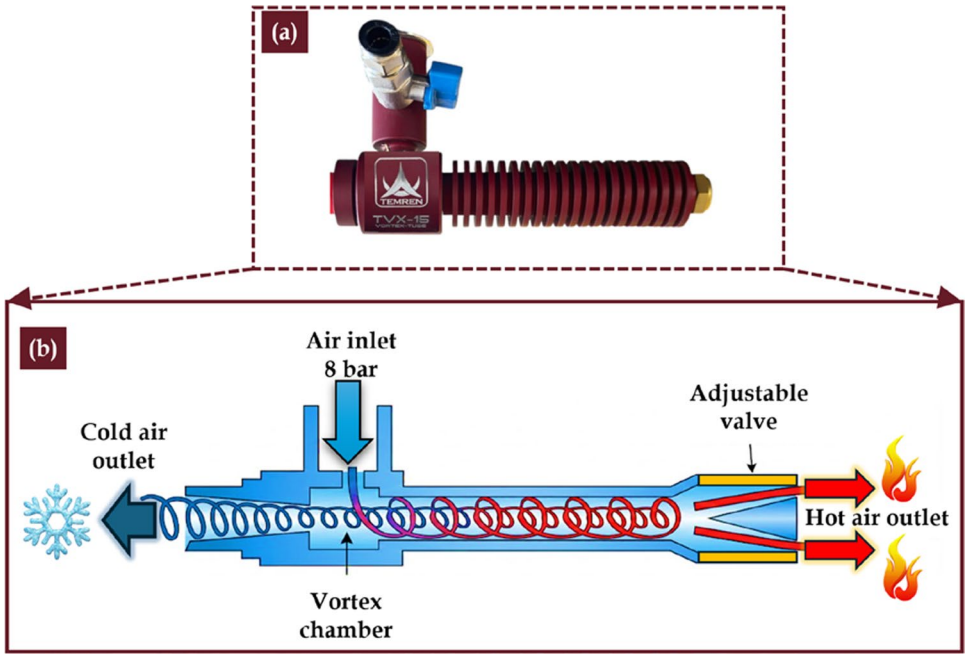

Fig. 2 Ranque–Hilsch vortex tube: **a** Temren TVX-15 and **b** schematic representation

air is split into two separate flows that rotate inside the tube. The RHVT system has two different outlets: one for high temperature and one for low temperature. A 3 mm-diameter nozzle was used to deliver cooled, dry air from the cold-air exit into the cutting zone. The RHVT system parameters (flow rate 20 mL/h, pressure 8 bar, nozzle diameter 3 mm, nozzle distance 20 mm, and nozzle angle 45 degrees) were consistent under all circumstances.

2.2.2 Preparation of surfactant-modified nanofluids

The goal of implementing sustainability in the machining sector is to reduce, or even eliminate, the use of petroleum-based cutting fluids. To this end, this study uses the MQL system, which has become widespread over the last 20 years as an alternative to conventional lubrication. The WERTE / STN 15 MQL system works by mixing the oil in the system with air from a compressor and applying the mixture to the cutting area via a nozzle. The air-oil mixture reaching the cutting area as an aerosol mist offers many advantages, including forming a tribofilm lubrication layer that aids plastic deformation, removing chips from the cutting area, and controlling cutting temperature. In this study, ester-based, rapidly biodegradable OPET Fuchs PlantoCut SR10 (kinematic viscosity: 10), specifically produced for machinability applications (i.e., turning, drilling, milling, etc.), with low evaporation properties and no H304, was selected as the base fluid. Using a two-step process, 0.6% by volume was added to improve the tribological characteristics of the vegetable-based oil. Throughout the experiments, the nanoparticle volume fraction was kept constant at 0.6% (by volume). This specific concentration was selected based on previous comprehensive optimization studies [58, 59], which demonstrated that values in the 0.5%–0.75% range provide the optimal balance between maximum thermal conductivity enhancement and critical colloidal stability, thereby effectively preventing issues such as significant agglomeration and nozzle clogging. The average size of CuO (Nanografi, Türkiye) nanoparticles is 38 nm, and they come in unique storage containers. SEM images of the CuO nanoparticles, particle size measurement results, EDS analysis, and properties are presented in Fig. 3. Freshly obtained nanoparticles from the container with the lid opened prior to mixing were used to prepare nanofluid mixtures using

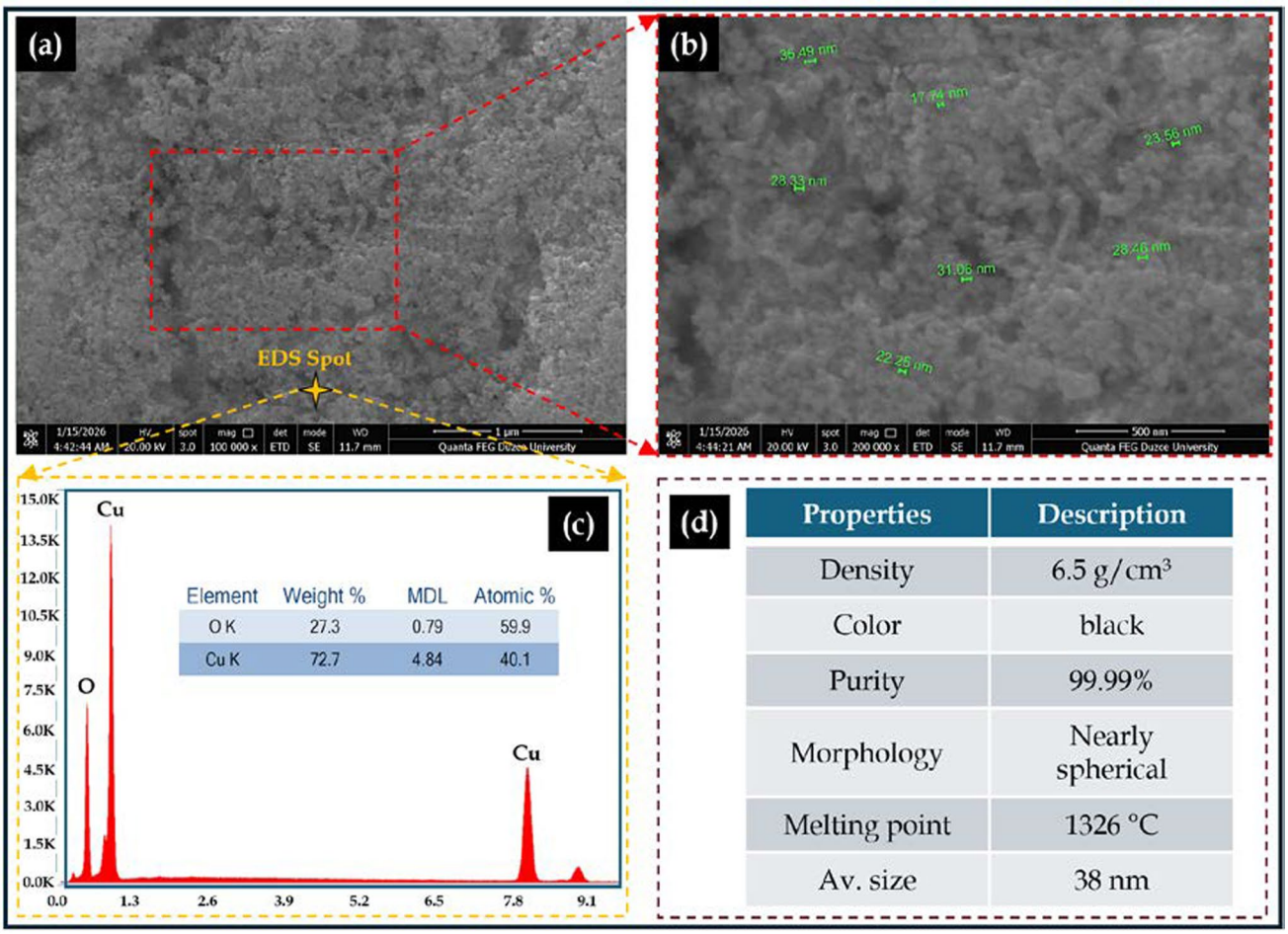

Fig. 3 CuO nanoparticles: **a** SEM images, **b** measuring particle sizes, **c** EDS analyzes, and **d** properties

appropriate mixing methods (namely, mechanical, ultrasonication, and magnetic stirrers, respectively).

Preserving the thermophysical properties of prepared colloidal nanofluid mixtures and maintaining long-term suspension stability are critical to tribological performance. Van der Waals forces cause nanoparticles to clump together and agglomerate in suspension mixtures due to their high surface areas and surface energy. This undesirable situation disrupts the nanofluid's homogeneity and leads to rapid sedimentation due to gravitational forces. By lowering the surface tension at the solid–liquid interface, surfactants in nanofluid mixes adsorb around nanoparticles and aid in the formation of an electrostatic or steric barrier [60].

In this study, surfactants with different chemical structures were added to the base fluid at fixed ratios to minimize nanoparticle agglomeration and optimize dispersion stability. Three different types of surfactants were selected to comparatively investigate their effects on the stabilization mechanisms in nanofluid mixtures: cationic Cetyltrimethylammonium Bromide (CTAB), anionic Sodium Dodecyl Sulfate (SDS), and nonionic Polyvinylpyrrolidone (PVP). SEM images and EDS analyses of SDS, PVP, and CTAB surfactants are presented in Fig. 4.

The preparation of nanofluid mixtures was carried out in four different stages. First, 0.6 percent of the vegetable oil was mixed with CuO nanoparticles. A mechanical mixer (Daihan HS 100D) was used to pre-mix the additional nanoparticles for ten minutes. Surfactants were added to the mixture at a concentration of 0.25% by weight of the nanoparticles, based on prior research and literature [61–63]. A mechanical stirrer was used to agitate the mixture for sixty minutes. In the second stage, the mixture was stirred for 30 min using a Bandelin SonoPuls HD3200 ultrasonic mixer. After 120 min of use with a Thermal N11151 M magnetic stirrer, nanofluid mixtures were obtained. The prepared nanofluid mixtures were used freshly in experimental studies without standing. The nanofluid preparation process is shown in Fig. 5.

2.3 Measurement and evaluation techniques

To determine the thermophysical measurements of the prepared nanofluid mixtures, viscosity measurements were first performed. Viscosity measurements were conducted at 40 °C. An oven was used to maintain a constant temperature. Viscosity measurements were performed in triplicate using an AND SV-10 viscometer at a constant volume of 50 mL. Prior to measurements, all probes were cleaned with isopropyl alcohol, and measurements were performed 5 min later. pH measurements were then performed. A Sartorius PT-10P pH meter was used to measure the pH three times. Device-specific cleaning and calibration procedures were used prior to each pH measurement of the nanofluid combination. Thermal conductivity was measured using a Decagon KD2Pro thermal conductivity meter. Nanofluid thermal conductivity was measured at 22 °C, and the probe was cleaned before each measurement to ensure calibration. Drop-point measurements are extremely important for investigating the wettability properties of nanofluid mixtures and for presenting the results in a striking manner. A device made by Biolin Scientific was used to measure drop points in this investigation. The workpiece was positioned on the device table with the Inconel X-750 surfaces parallel to each other prior to the measurements. Three separate measurements from different parts of the workpiece surface were averaged in the room-temperature experimental investigation.

To obtain thermographic images for the experimental study, an Optris PI 450 infrared camera, with a measuring range of −20 to 900 °C and a frame rate of 80 Hz, was placed 300 mm from the cutting zone. Prior to measurement, the instrument was calibrated using the manufacturer's online verification. The emissivity value for thermal camera measurements was set to 0.42 based on the device manufacturer's catalog values and literature research [57, 64]. Surface quality is critical to machinability. The average surface roughness (Ra) was considered a surface quality attribute of sustainably milled surfaces under various conditions in this study. All measurements were performed in accordance with ISO 21920–3:2021. Arithmetic mean values were computed from measurements made from three distinct areas of the milled surfaces: the area where the cutting tool enters the workpiece, the area where the cutting tool exits the workpiece, and the machined middle area. Cutting force or device power consumption parameters are often used to verify that different sustainable conditions reduce carbon emissions. In this study, however, the power consumption during milling under different conditions was recorded using a Fluke 1732 energy logger with three-channel measurement capacity. The idle power consumption of the CNC vertical machining center was measured, and the actual consumption was determined by subtracting the data collected during milling. Using a Dino-Lite AM73915MZT4 digital microscope, the wear levels of the cutting tools were measured. The cutting tool flank wear was measured in accordance with ISO 3685:1993. Cutting tool wear mechanisms were identified, and nanoparticles and surfactants were measured with an FEI Quanta FEG250 SEM. To ensure statistical reliability and reproducibility of the experimental findings, all milling experiments and subsequent measurements (including surface roughness, cutting temperature, and power consumption) were repeated three times under identical conditions. While the data presented in the results section represent the arithmetic mean of these replicates, the

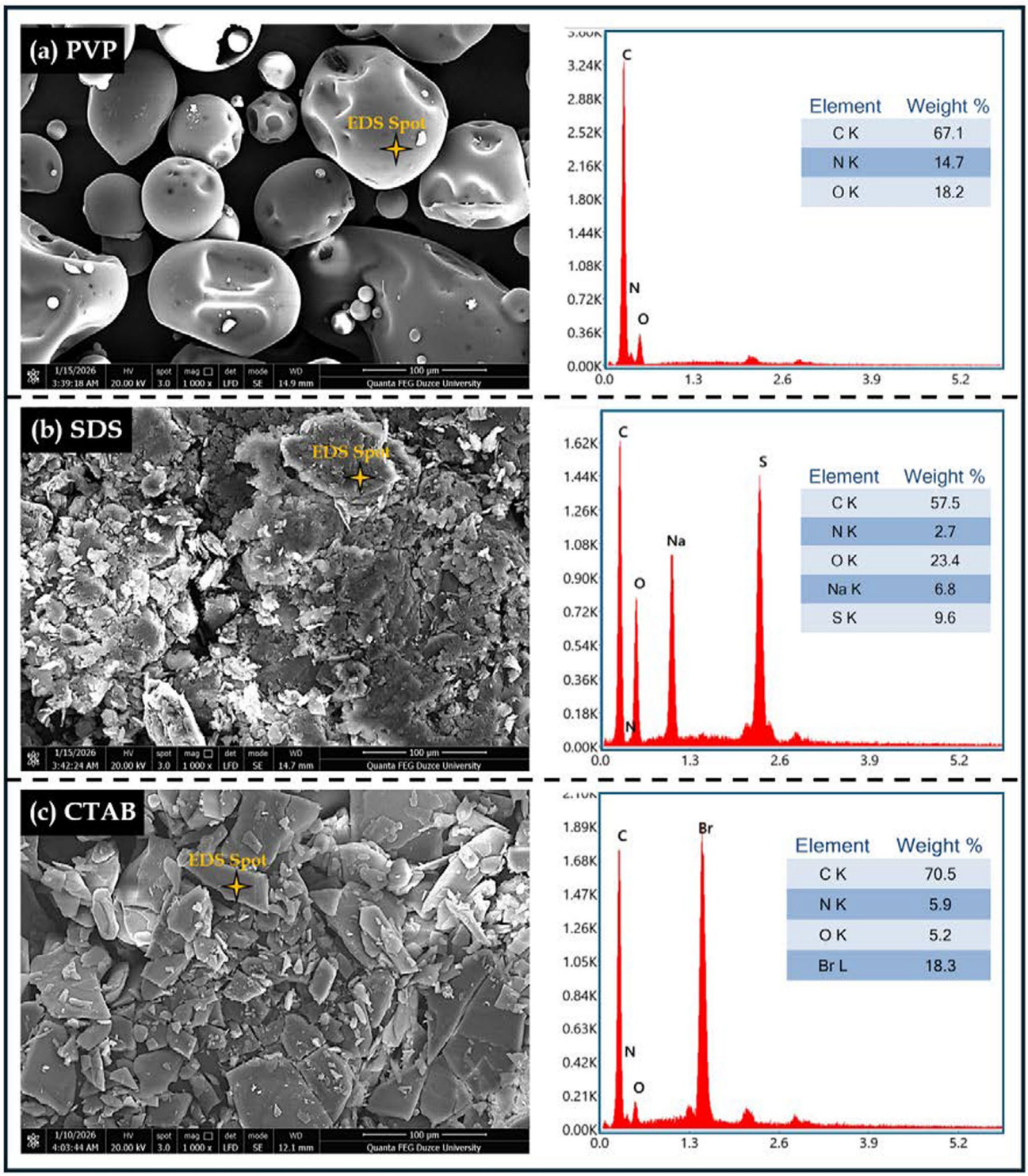

Fig. 4 Surfactants SEM images and EDS spot analyzes: **a** PVP, **b** SDS, and **c** CTAB

error bars in the corresponding graphs indicate the standard deviation (±SD). Figure 6 shows a detailed schematic of the experimental setup, and Table 1 presents the experimental specifications.

3 Results and discussion

The true efficacy of the proposed hybrid thermal management framework must be interpreted by correlating the intrinsic physical properties of the developed fluids with

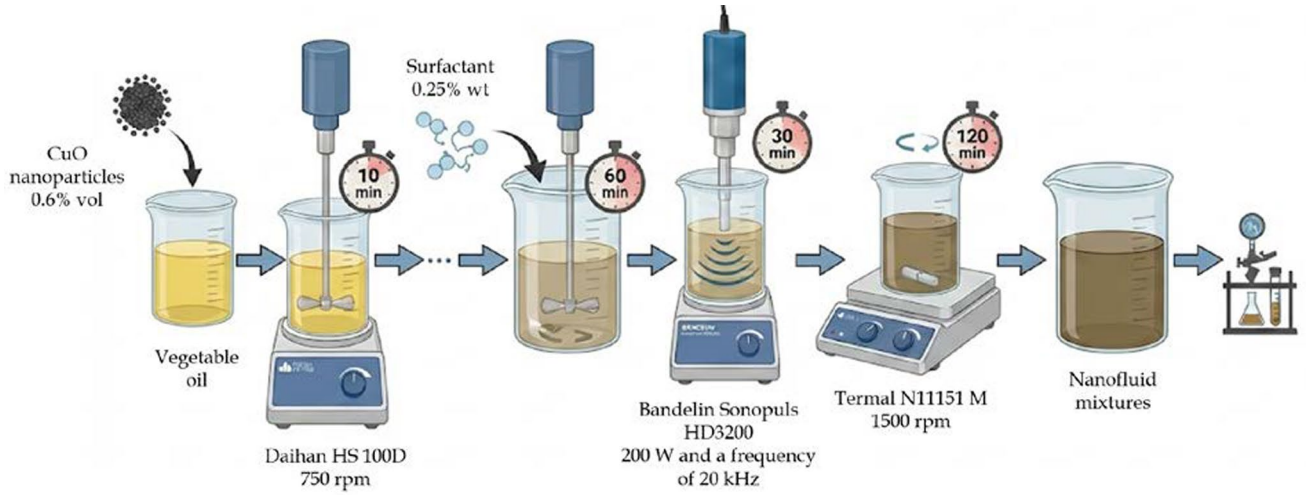

Fig. 5 Nanofluid preparation processes

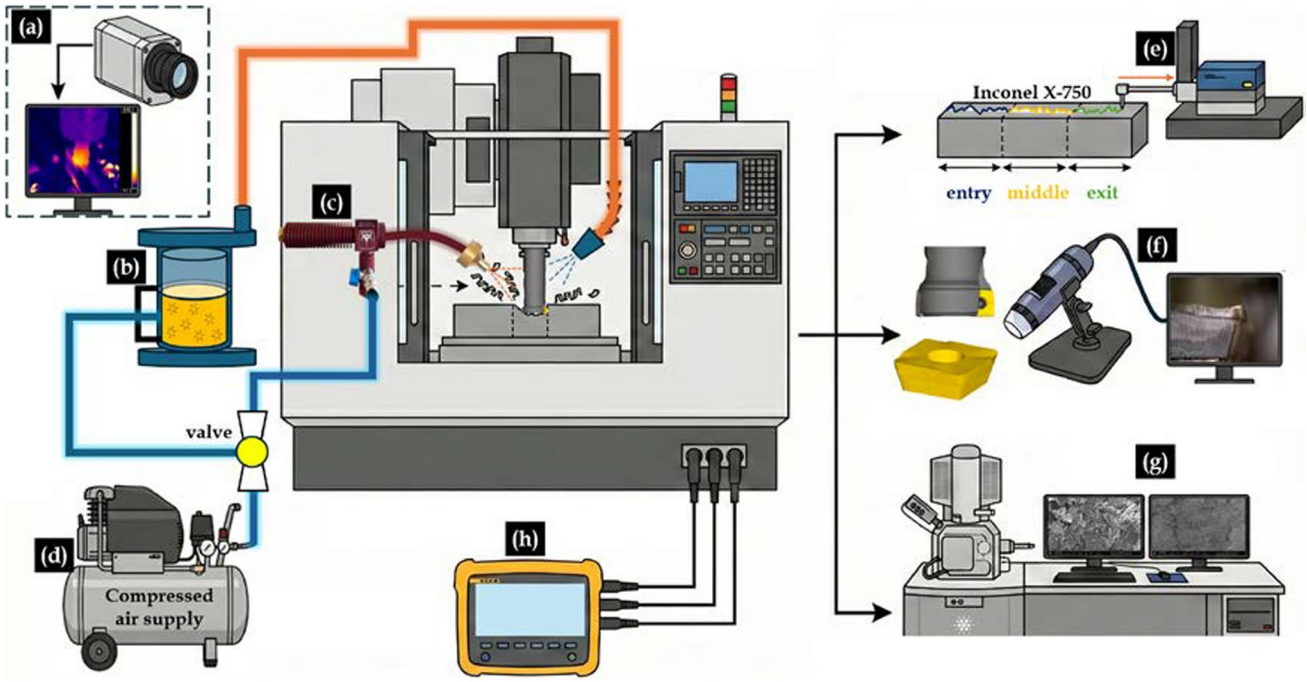

Fig. 6 Experimental representation: **a** Thermal imager, **b** MQL supply system, **c** RHVT vortex, **d** Compressor, and analyze for **e** Surface roughness, **f** Flank wear, **g** SEM wear mechanisms, and **h** Power logger

their dynamic behavior in the machining zone. Accordingly, this section initially analyzes the thermophysical characteristics and wettability of the surfactant-modified CuO nanofluids to establish a functional baseline for their cooling and lubricating potential. Building upon this fluid characterization, the subsequent subsections systematically evaluate how these fluids—when coupled with cryogenic vortex air—govern the actual milling performance of Inconel X-750. The comprehensive discussion is structured around the evolution of cutting temperatures, resultant surface integrity, variations in power consumption, and the dominant tool wear mechanisms propagating under severe mechanical loads.

3.1 Thermophysical properties of nanofluids

This section presents a comprehensive evaluation of the experimental findings. First, the thermophysical properties of the formulated nanofluids are analyzed to understand their base characteristics. Subsequently, the effects of these fluids and hybrid cooling conditions on cutting temperature, surface roughness, power consumption, and tool wear

Table 1 Experimental specifications

Parameter	Specifications
Machining center	Delta SEIKI CNC1050 A
Workpiece material	Inconel X-750
Holder	490-025A20-08L, Sandvik
Cutting tool	490R-08T308E ML, Sandvik
Milling parameters	Vc 70 m/min, f 0.2 mm/rev, and ap 0.5 mm
Vortex cooling system	Temren TVX-15, Tecus
Vortex setup values	flow rate 20 mL/h, pressure 8 bar, nozzle diameter 3 mm, and nozzle angle 45 degrees
MQL system	STN 15, WERTE
MQL setup values	input pressure 4–6 bar, flow rate 40 mL/h, nozzle diameter 2 mm, and nozzle angle 45 degrees
Surfactants	SDS, PVP, and CTAB
Basefluid	OPET Fuchs PlantoCut SR10
Cooling/lubrication environments	dry[1], vortex[2], MQL[3], MQL+vortex[4], CuO[5], CuO+vortex[6], CuO/PVP[7], CuO/PVP+vortex[8], CuO/SDS[9], CuO/SDS+vortex[10], CuO/CTAB[11], CuO/CTAB+vortex[12]

mechanisms during the milling of Inconel X-750 are systematically discussed.

3.1.1 Viscosity and pH

The viscosity of nanofluids is a physicochemical property that determines the fluid's internal frictional resistance to flow and directly affects the performance of thermal systems. While it is known that the heat transfer efficiency of nanofluids is related to thermal conductivity, their viscosity is another parameter that affects this efficiency [65]. Therefore, to fully establish the relationship between processing performance and fluids, it is essential to know the viscosity of the fluids used in the cutting process. Because of this, the viscosity of the fluids used during cutting was tested in this phase of the study, and the findings are shown in Fig. 7. The base fluid had the lowest viscosity, 10.4 mm^2/s, as seen in Fig. 7. Nevertheless, the viscosity value climbed by 8.65% to 11.3 mm^2/s when the CuO nanoadditive was added to the base fluid. By improving particle–particle and particle-base-fluid interactions, the addition of nanoadditives to the base fluid raises viscosity. By changing the fluid's laminar or turbulent flow properties, this increase in viscosity significantly affects the convective heat transfer coefficient and total heat transfer performance [66]. Another observation in Fig. 7 is that viscosity continues to increase as surfactants are added to the nanofluid. Compared to the base fluid, the viscosity values of CuO/PVP, CuO/SDS, and CuO/CTAB nanofluids increased by 14.42%, 16.35%, and 19.23%, respectively. The reorganization of particle-base fluid and particle–particle interactions at the nanoscale has been linked to the rise in viscosity that occurs when surfactants are added. According to Wang et al. [67], the addition of surfactant enhanced the viscosity of nanofluids, which was consistent with the current study's prediction. This increase was linked to the adsorption of surfactant molecules onto the nanoparticles' surfaces, thereby increasing the hydrodynamic diameter and strengthening particle–fluid interactions.

The pH value in nanofluids is a logarithmic measure of hydrogen-ion activity. Furthermore, pH is of great importance for stability and consistency, as it determines the electric double layer and the surface charge distribution between the nanoparticles and the carrier fluid. The correct pH value increases the zeta potential, prevents agglomeration of the nano-additive particles, and ensures homogeneous

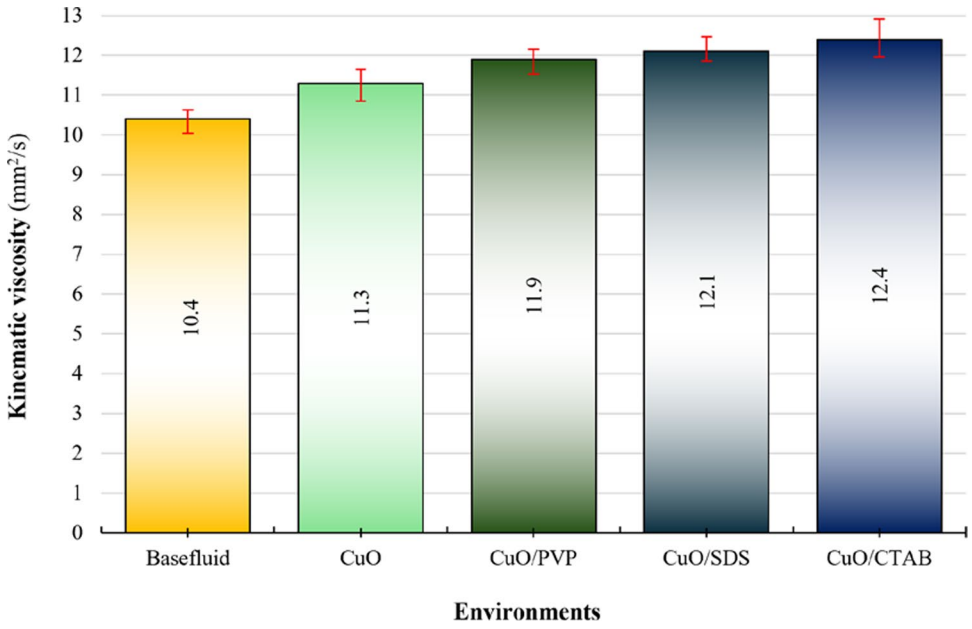

Fig. 7 Viscosity results value of different lubrication strategies (at 40 °C)

dispersion [68, 69]. Furthermore, adjusting the pH value to the correct level reduces sedimentation and flocculation, while also altering the thermophysical properties of the fluid [37]. In particular, it is of interest to examine how pH changes with the addition of surfactants. To evaluate the impact of the additives on pH, pH values were measured for several surfactant-containing nanofluids, the surfactant-free nanofluid, and the base cutting fluid in this phase of the study. Figure 8 displays the pH values derived from these experiments. The base fluid had the lowest pH reading, 5.537. The pH of the base fluid increased to 5.765 upon addition of nano-CuO. Stated otherwise, there was a 4.12% rise in pH. Metal oxide nano solid lubricants such as CuO can release a certain amount of Cu^{2+} ions into the environment or rearrange the ionic equilibrium in the solution by forming surface hydroxide complexes, which can contribute to a net pH increase with a shift towards a basic environment [70]. Nevertheless, the pH of the nanofluid continued to rise after the addition of surfactants. Compared to the base cutting fluid, the pH value of the PVP, SDS, and CTAB surfactant-containing CuO nanofluid increased by 8.81%, 8.52%, and 6.18%, respectively. The ionic nature of the surfactants helps to explain this. Nanofluid stability can be improved by using ionic surfactants such as SDS and CTAB, or nonionic surfactants such as PVP. These surfactants can have different effects on the pH value depending on their structure. Non-ionic surfactants such as PVP act via steric stabilization, exhibiting a more stable zeta potential over pH changes, while ionic surfactants such as SDS and CTAB can modify particle–particle and electrostatic interactions by more significantly affecting the ionic equilibrium in solution and, consequently, the zeta potential. Non-ionic surfactants act through the steric stabilization mechanism and can provide a more stable zeta potential behavior against pH changes [69].

3.1.2 Thermal conductivity

The cutting action and associated friction in metal-cutting operations generate significant heat. This heat, however, must be quickly removed from the cutting zone to maximize machining efficiency. When machining high-strength, low-thermal-conductivity materials, such nickel-based superalloys, heat dissipation is especially challenging [71]. For this reason, the use of cutting fluids is quite popular. Here, the heat-transfer capacity of the cutting fluids is important, and their thermal conductivity is measured to determine it. Thermal conductivity measurements not only determine cooling efficiency and heat transfer capacity but also enable us to understand the effects of micro-scale mechanisms such as nanoparticle-fluid interactions, particle dispersion, Brownian motion, and microconvection [72, 73]. Therefore, the base cutting fluid and the nanofluids employed in this study were measured for their thermal conductivities. The goal was to investigate the relationship between the fluids' thermal conductivity ratings and the experimental findings. Figure 9 displays the findings of the thermal conductivity measurement conducted for this purpose. The base cutting fluid had the lowest thermal conductivity, 0.163 W/m · K, as shown in Fig. 9. However, adding nano-sized CuO to the base cutting fluid significantly increased its thermal conductivity. In fact, the thermal conductivity increased by 201.84% compared to the basic cutting fluid. Due to the high surface/volume ratio of nanoparticles, the thermal conductivity of nanofluids is much higher than that of base fluids or microfluids [74]. Furthermore, owing to their superior

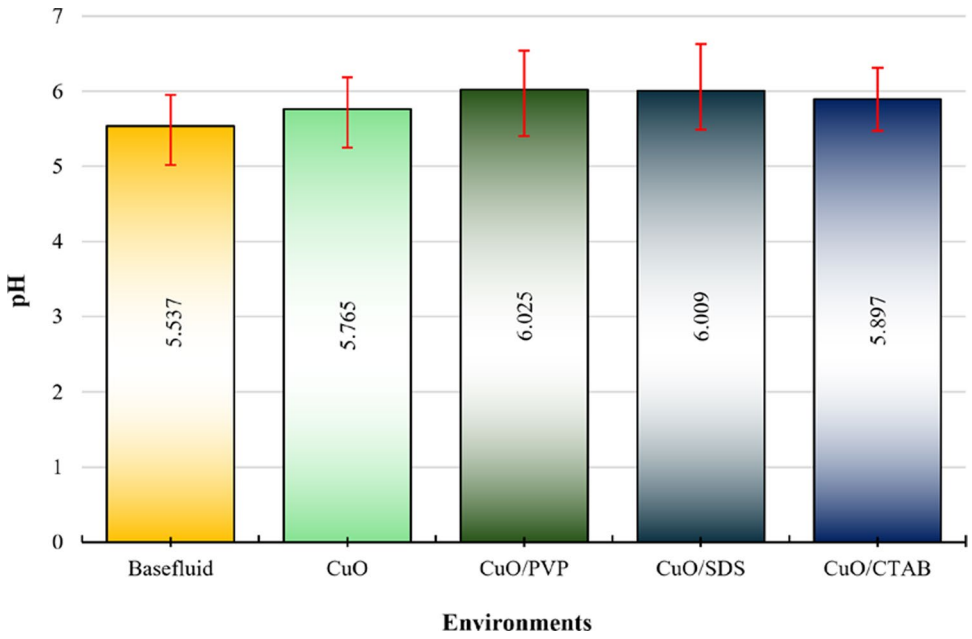

Fig. 8. pH results value of different lubrication strategies

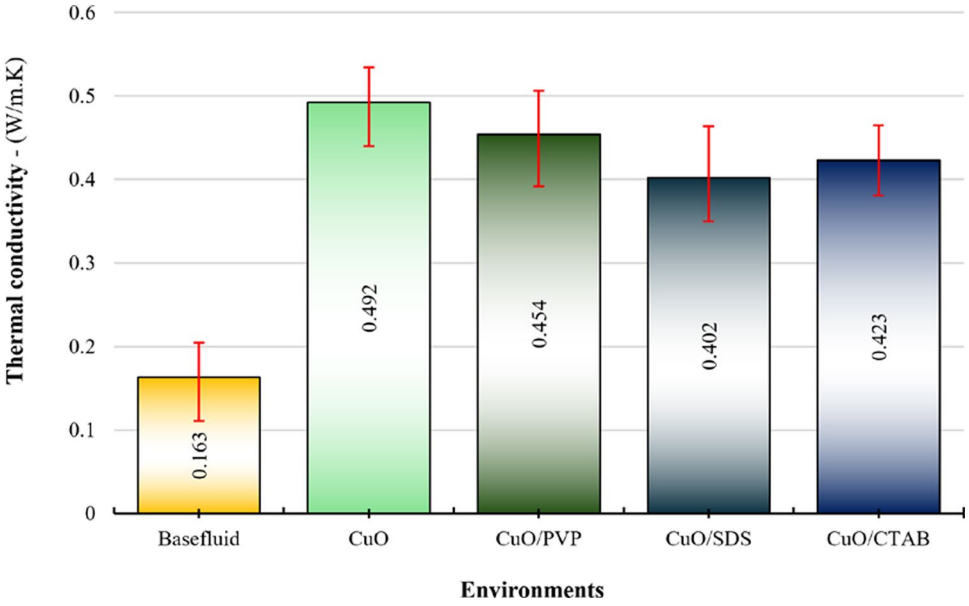

Fig. 9 Thermal conductivity values under different cooling/lubrication environments

qualities, including strong electrical insulation, high thermal conductivity, good compatibility with base fluids, and a high cost-performance ratio, metal oxides are widely used in nanofluids [75]. Metal oxides are preferred in many applications that require high thermal conductivity due to their favorable performance [76]. The significant increase in thermal conductivity is consistent with recent phenomenological studies in the literature demonstrating that well-dispersed metal oxide nanoparticles fundamentally alter the thermophysical dynamics and heat-transfer capacity of the base fluid [77, 78]. CuO's high surface area, electrical conductivity, and capacitance, all of which result from its distinct structural characteristics have attracted significant attention [79]. Additionally, when used as an additive in nanofluids, it performs exceptionally well, increasing thermal conductivity. Sivakuma et al. [80] reported that adding nano-CuO to an ethylene glycol-based fluid significantly increased its electrical conductivity. However, adding surfactants to the CuO-containing nanofluid resulted in a small drop in thermal conductivity. Compared to the surfactant-free CuO-containing nanofluid, the thermal conductivity values of the CuO/PVP, CuO/SDS, and CuO/CTAB nanofluids decreased by 7.72%, 18.29%, and 14.02%, respectively. The stability and thermal conductivity of nanofluids can be improved by adding surfactants. However, the literature often emphasizes that surfactants added in incorrect proportions reduce thermal conductivity [81, 82]. Another notable finding from thermal conductivity measurements is that the highest thermal conductivity was observed in PVP-containing surfactant nanofluids. This situation supports the processability results (Sects. 3.2, 3.3, 3.4, and 3.5).

3.1.3 Contact angle of fluids

The contact angle characterizes the equilibrium geometry between a solid surface and a liquid droplet. This angle is derived from Young's equation and describes the surface's hydrophilic or hydrophobic behavior. The contact angle changes, particularly with the addition of nanoparticles and surfactants [83]. A direct quantitative indicator of a nanofluid's interaction with a surface, the contact angle influences important machining (chip removal) processes such heat transfer, lubricant film generation, and the tribofilm/mending behavior of nanoparticles [84–86]. It is an important indicator because it determines film formation at wettable and sliding surfaces, the ability of the liquid to penetrate the contact surfaces, and the mechanisms by which the liquid exerts thermal and tribological effects [87, 88]. Therefore, contact angle measurements are indispensable for the development of nanofluids and MQL applications, including formulation optimization, mechanism analysis, and process parameter design. Additionally, the contact angle quantifies the lubricating capacity of the nanofluid [83]. It is a standard measurement parameter that indicates lubrication capability, especially when evaluated alongside other parameters such as thermal conductivity and viscosity. It is also a crucial figure for forecasting the efficacy of lubrication in practical settings. In light of these considerations, contact measurements were made on the nanofluids employed in this investigation; the results are shown in Fig. 10. Thus, the lubrication ability of the base MQL fluid, the nanofluid, and the surfactants added to the nanofluid was demonstrated. According to Fig. 10, the lowest contact angle was observed with the pure MQL fluid at 4.530º. Adding solid lubricant to the base cutting fluid resulted in an increase in contact

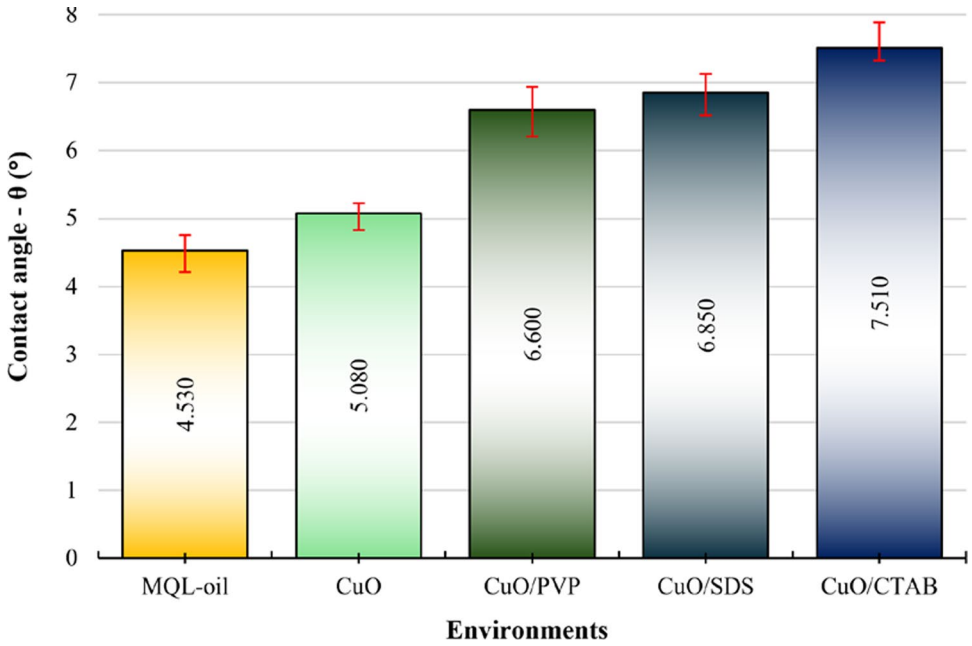

Fig. 10 Contact angle results under different cooling/lubrication environments (Error bars represent the standard deviation of three repeated measurements)

angle. This increase reached 12.14%. Vafaei et al. [89] also stated that changes in particle size and/or concentration ratio could increase or decrease the contact angle. Furthermore, the contact angle continued to increase with the addition of surfactant to the nanofluid. Compared to the surfactant-free nanofluid, the contact angle increased by 29.92%, 34.84%, and 47.83% for CuO/PVP, CuO/SDS, and CuO/CTAB, respectively. This was attributed to the properties of the particles and surfactants. It is thought that the fact that all additives change the contact angle to different degrees is also related to these structural relationships. According to Wen et al. [90], the accumulation of hydrophobic nanoparticles or surfactant-particle complexes at the three-phase contact line can stabilize the edge of the droplet and prevent spreading. Furthermore, the particle layer on the surface can alter the apparent surface chemistry and increase effective hydrophobicity. Therefore, additives or surfactants added to the base liquid can increase the liquid's contact angle.

3.2 Cutting temperature evaluation

About 90% of the mechanical energy is converted to thermal energy during chip removal, causing the cutting zone to become very hot [91]. Excessive wear on the tool rake and flank faces results from uncontrolled high cutting temperatures. As a result, tool life might be greatly decreased [92]. Furthermore, the induced thermal softening of the tool-workpiece pair disrupts chemical element diffusion and causes deterioration of the machined surface [93]. In addition, cutting temperature is also critical for dimensional accuracy and geometric deviations. Therefore, it is very important to keep it under control [94, 95]. A lubrication/cooling system is one of the most popular methods for regulating cutting temperature. Thus, the impact of eleven distinct cooling techniques on cutting temperature was examined in this phase of the study. To assess how these cooling techniques affected cutting temperature, dry machining was incorporated into the experimental design. Figure 11 illustrates how the cutting temperature changes with various cooling techniques. Under dry machining, the highest cutting temperature was 323 °C; with cooling strategies, the decrease in cutting temperature varied by method. This situation is related to the effectiveness of cooling/lubrication methods in the cutting process. Depending on the strategy's dynamics, cooling/lubrication methods either reduce friction by providing effective lubrication and minimizing cutting temperature at the moment of formation, or by ensuring that the heat generated is quickly dissipated from the cutting area [96]. However, the change in cutting temperature may vary depending on the characteristics and power of the cooling strategy used. For example, vortex cooling reduced the cutting temperature by 15.79%, while pure MQL lubrication reduced it by 19.81%. The decrease in cutting temperature with the vortex tube can be explained by a reduction in thermal load in the cutting zone, resulting from increased convective heat transfer [97]. The decrease in cutting temperature with MQL can be explained by the small amount of oil delivered by compressed air that penetrates the tool-chip-workpiece interface, forming an oil film that reduces friction. Furthermore, in the hybrid system (MQL+vortex), the decrease in cutting temperature was 25.39%, indicating that both cooling and lubrication were more effective. With the addition of nanofluids, the cutting temperature continued to drop. The use of CuO-containing nanofluid reduced the cutting

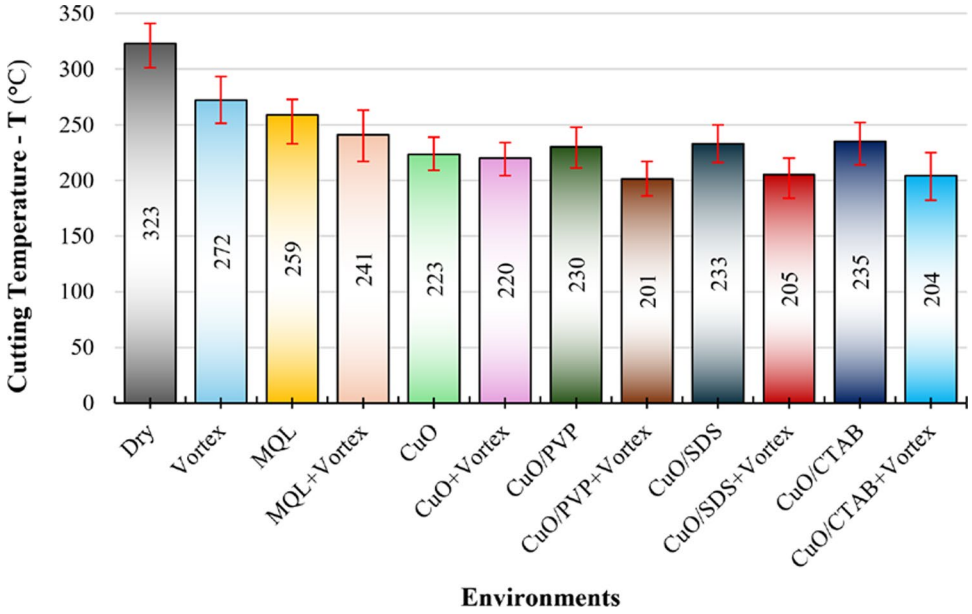

Fig. 11 Cutting temperature results under different cooling/lubrication environments (Error bars represent the standard deviation of three repeated measurements)

temperature by 30.96% compared to dry machining. This is explained by the fact that nanofluids efficiently dissipate heat from the cutting zone, thereby reducing mechanical output. Nanofluids, which offer higher thermal conductivity than the basic cutting fluid, can be used to quickly remove heat from the cutting zone and form tribofilms that reduce heat generation [98]. However, adding a surface additive to CuO-containing nanofluids increased cutting temperatures. Compared to CuO-doped nanofluids, the addition of PVP, SDS, and CTAP surfactants increased the cutting temperature by 3.14%, 4.48%, and 5.38%, respectively. This was attributed to changes in thermal conductivity and viscosity associated with surfactant addition. Keklikçoglu [99] emphasized that the addition of surfactants reduces the thermal conductivity of GO/water nanofluids. In another study, Sajid et al. [100] reported a decrease in thermal conductivity, especially at high surfactant concentrations. Again, some studies report that nanofluid performance decreases with the surfactant-nano additive's dose/type compatibility [101, 102]. However, when surfactant-additive nanofluids were used together with a vortex tube, the cutting temperature decreased. In fact, these cooling conditions provided the lowest cutting temperatures in the entire experimental design. Compared to dry cutting, the reductions in cutting temperature under the CuO/PVP+vortex, CuO/SDS+vortex, and CuO/CTAB+vortex conditions were 37.77%, 36.53%, and 36.84%, respectively. In this combination, improved atomization, droplet distribution, wetting, and nanoparticle stabilization may contribute to reduced temperature by enhancing oil-mist interaction. Furthermore, blowing cold air into the cutting zone via vortex reduces thermal conductivity due to surfactants [52]. The high-speed cryogenic air supplied by the vortex tube effectively suppresses localized thermal gradients and delays the onset of the Leidenfrost effect [103]. By preventing evaporation, this process enables the formation of an effective tribofilm layer, as the sub-zero convective cooling preserves the structural integrity of the surfactant-modified CuO nanofluid droplets.

3.3 Surface roughness evaluation

The roughness resulting from the metal-cutting process is directly related to stress concentrations, microcrack formation, and, consequently, the fatigue behavior of materials [104]. In addition, the surface marks and microgeometry can provide a substrate for the formation of corrosion cells. Micro-pits and surface irregularities cause localized corrosion. Therefore, surface roughness is a critical output parameter for applications requiring corrosion resistance [105, 106]. In addition, the quality of the machined surface is very important in many areas, including assembly, sealing, coating efficiency, production costs, and compliance with standards [107, 108]. For all these reasons, measuring and improving surface quality is always a topic of interest in machining operations. Achieving surface integrity and extended tool life is a primary objective in the machining of advanced engineering materials. Recent and comprehensive studies in literature have successfully demonstrated that statistical optimization techniques, particularly Analysis of Variance (ANOVA), are highly effective tools for determining optimal machining parameters and understanding their effects across various materials [109]. The present study relies primarily on phenomenological mechanism analysis and standard deviation (error bars) to validate the reliability of the synergistic hybrid vortex-nanolubrication environment. The impact of various cooling techniques

on the average surface roughness (Ra) was investigated in this phase of the study; the findings are shown in Fig. 12. The highest Ra value was observed under dry machining at 0.470 µm. A decrease in the Ra value was observed when cooling methods were used. For example, while the Ra value decreased by 22.77% under vortex conditions, it decreased by 26.6% with MQL use. High temperatures during dry cutting and thermal softening at the tool-chip interface increase flow and plastic deformation. This increases both cutting-edge deformation and surface microstructural damage, thereby increasing surface roughness. Cooling mitigates these thermal effects, while lubrication reduces friction at the interfaces. Thus, cutting temperature, cutting forces, ploughing effect on the surface, and BUE formation are limited [110–113]. This results in easier cutting and a smoother surface. Furthermore, the introduction of cutting fluids containing nanolubricants has led to greater improvements in surface roughness. Compared to dry processing, the use of CuO-added nanofluid reduced the Ra value by 49.36%. This is attributed to the positive changes in the fluid's thermal and tribological behavior upon addition of the nanoadditive. CuO particles quickly dissipate the high heat in the cutting zone by increasing the carrier fluid's thermal conductivity [29]. Shabgrad et al. [114] compared dry, conventional lubrication, MQL, and CuO-added nanofluids at different concentrations for the grinding of hardened AISI 1045 steel at varying feed rates and chip depths, and reported that the nanofluid showed promising results. However, adding surfactant to the nanofluid caused a slight increase in the Ra value. This increase was observed in all three surfactant types, albeit at different rates. Compared to the surfactant-free CuO-containing fluid, the Ra value increased by 1.26%, 7.14%, and 2.94% when using CuO/PVP, CuO/SDS, and CuO/CTAP fluids, respectively. This was explained by the surfactants' ability to lower atomization, viscosity, and heat conductivity. The use of surfactants may reduce the fluid's thermal conductivity, increase local softening, and increase BUE [115]. Fazeli et al. [116] reported that adding surfactants to CuO-doped nanofluids can reduce thermal conductivity, consistent with the prediction in this study. Furthermore, the wrong surfactant type and/or a suboptimal concentration ratio may have led to nanoparticle aggregation or, conversely, excessive stabilization, thereby preventing the desired tribofilm formation [117]. Interestingly, however, the Ra value decreased again under cooling conditions when surfactant-doped nanofluids were used in conjunction with a vortex tube. In fact, these circumstances produced the lowest Ra value across the entire testing set. Compared to the CuO condition, the Ra value decreased by 8.82% with CuO+vortex, while compared to CuO/PVP, CuO/PVP+vortex showed a 29.88% improvement, compared to CuO/SDS, CuO/SDS+Vortex showed a 20.78% improvement, and compared to CuO/CTAB, CuO/CTAB+vortex showed a 15.51% improvement. The cooling effect of the vortex tube has been linked to this circumstance. The combination of cold air jet from the vortex tube and CuO-nanofluid stabilized with surfactant compensates for the negative effects of surfactant alone (e.g., atomization/penetration breakdown, adverse changes in local heat transfer, residue formation on the surface) [118].

3.4 Power consumption analysis

The cutting force and total energy consumed during chip removal are directly related to labor and part costs, as well as production efficiency [119]. Furthermore, it increases

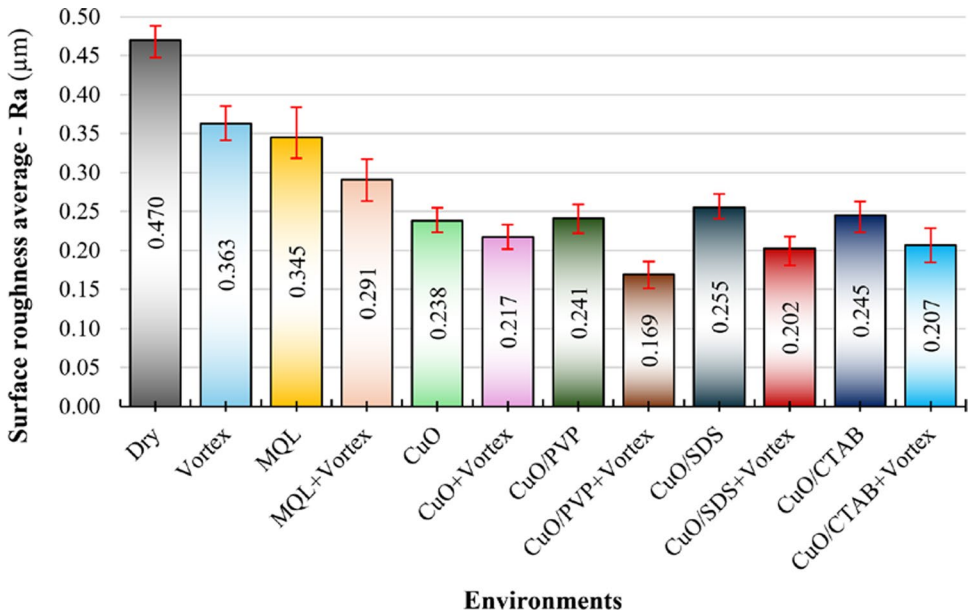

Fig. 12 Surface roughness results under different cooling/lubrication environments

electricity-related carbon emissions depending on the amount of energy consumed during chip removal. In other words, energy consumption directly affects the effort required to achieve the "green production" goal [120]. However, the energy consumed during chip removal is generally calculated theoretically, and costs are determined accordingly. But theoretical calculation models may deviate due to differences in laboratory facilities and machine-workpiece interactions. Therefore, it must be measured directly, and energy consumption must be reduced [121]. Reducing energy consumption can lower production and maintenance costs while increasing efficiency [122]. It can also help reduce the carbon footprint and achieve sustainability goals [123]. In conclusion, reducing the energy consumption used in metal cutting is critical in many ways. One of the most fundamental ways to achieve this is to facilitate cutting. At this point, using cooling systems is a recommended approach. However, since many cooling methods are currently used during cutting, determining the best strategy is critical. In this section of the study, several cooling strategies were compared, and their effects on power consumption are shown in Fig. 13. The goal was to identify the best cooling plan in terms of electricity usage. The maximum power consumption of 380 watts was observed in dry conditions, as shown in Fig. 13. Dry cutting results in significantly greater friction. The thermal load is increased by heat that is collected as a result of friction at the tool-chip-workpiece contacts. This load increases the cutting force and, as a result, energy consumption [124]. Additionally, due to this high friction, the contact time between the tool tip and the chip may be longer. This makes cutting more difficult, thereby increasing energy consumption [125]. With the introduction of cooling conditions, energy consumption has decreased. For example, energy consumption decreased by 4.47% with vortex tubes and by 7.89% with MQL. This is attributed to the positive effect of lubrication and cooling systems on cutting. Cooling and lubrication improve tool-chip-workpiece interaction by reducing friction and cutting-zone temperatures. As a result, cutting forces and cutting energy decrease, tool wear slows, process stability increases, and, consequently, power consumption decreases [126–128]. When cooling and lubrication are used together under MQL+vortex conditions, the reduction is even greater, reaching 13.16%. When the vortex tube, known for its cooling properties, and MQL, which emphasizes lubrication, are used together, both cooling and lubrication are performed effectively, improving cutting performance. With improved cutting performance, cutting is easier and consumes less energy. When a nano additive is added to the cutting fluid, the decrease in total energy consumption continues. Compared with pure MQL, the energy consumption of the CuO-added nanofluid decreased by 7.14%. The nanoparticles in the nanofluid form a tribofilm on the contact surfaces or create a continuous boundary-lubricating layer. This coating lowers friction and stops metal-to-metal contact. As a result, lower tangential force and lower power consumption are achieved [85, 129]. Surfactants added to nanofluids also contributed to reduced power consumption. Compared to surfactant-free nanofluids (CuO), surfactant-containing nanofluids CuO/PVP, CuO/SDS, and CuO/CTAB provided 4.62%, 6.46%, and 5.23% lower power consumption, respectively. Surfactant addition can improve cutting by enhancing stability, penetration, and atomization, thereby improving thermal-tribological properties and reducing power consumption [66]. However, the lowest power consumption was observed when surfactant-containing nanofluids were used with a vortex tube. For

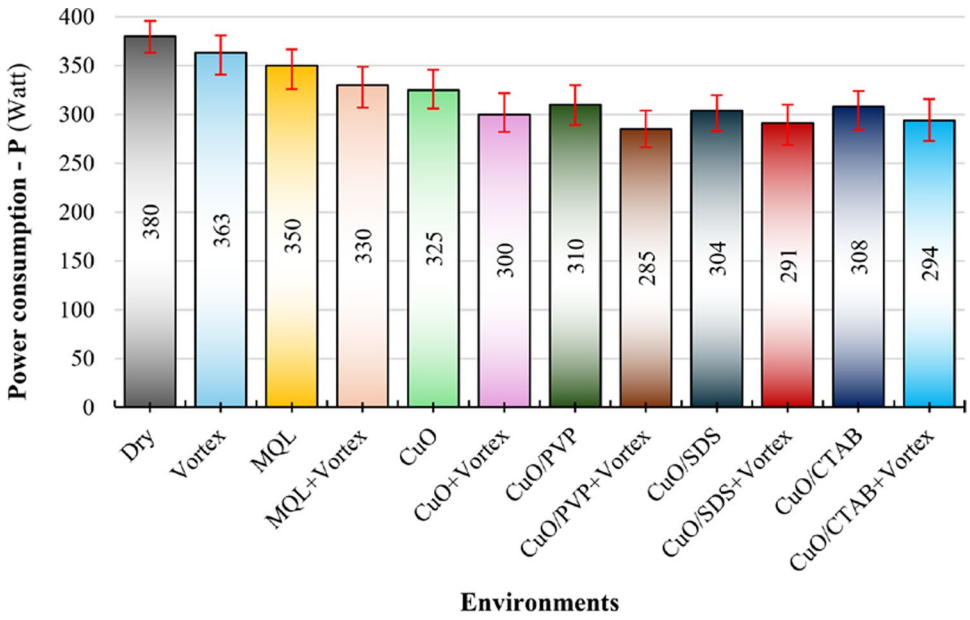

Fig. 13 Power consumption results under different cooling/lubrication environments

example, compared to CuO/PVP, CuO/PVP+vortex reduced power consumption by 8.06%, compared to CuO/SDS, CuO/SDS+vortex reduced it by 4.28%, and compared to CuO/CTAB, CuO/CTAB+vortex reduced it by 4.55%. This is attributed to the combined improvement effect on cutting achieved by the simultaneous use of stable lubrication and cooling. In fundamental machining operations, mechanical power consumption is directly proportional to the primary cutting forces acting at the tool-workpiece-chip interface. Recent studies in the literature, such as those evaluating the machinability of advanced silicon nitride-reinforced composites [131], have clearly demonstrated that the presence of solid micro- and nano additives can significantly alter interfacial friction and reduce cutting forces. When this mechanistic principle is applied to the present study, the lubricating tribofilm layer formed by surfactant-modified CuO nanoparticles effectively reduces shear stress and frictional resistance in the secondary shear zone. Although cutting forces were not measured directly in real time, they are considered a direct, factual indicator that primary cutting forces were substantially reduced by this synergistic hybrid cooling approach. Beyond thermomechanical and tribological improvements, the proposed hybrid CuO/PVP+vortex system demonstrates potential for sustainable and cleaner manufacturing. Compared to conventional flood cooling methods that consume large volumes of lubricant, the MQL system, characterized by extremely low fluid consumption (40 mL/h) and the use of clean vortex air, eliminates significant ecological concerns. Furthermore, the 25% reduction in power consumption during machining directly translates to a lower carbon footprint and reduced greenhouse gas emissions. Consequently, this eco-friendly strategy offers a highly viable, energy-efficient, and environmentally conscious solution for the sustainable machining of advanced aerospace superalloys such as Inconel X-750.

3.5 Tool wear mechanisms and tool life

During machining, cutting tools are exposed to high temperatures, high pressures, and shear stresses. Under these demanding conditions, the mass loss at the cutting edge is called tool wear and primarily occurs through adhesion, abrasion, diffusion, and oxidation mechanisms [131]. Flank wear, in particular, is one of the most important types of wear that can characterize tool wear. The cutting wedge radius increases as the cutting edge's macrogeometry deteriorates due to tool wear. After this stage, shearing and crushing occur rather than cutting. Furthermore, this geometric distortion leads to increased surface roughness [132]. A worn cutting tool causes more plastic deformation and instability on the workpiece surface, resulting in degraded surface quality and dimensional tolerances [133]. When examining the effects of tool wear on cutting temperature, dulling at the cutting edge can dramatically increase temperatures in the cutting zone by increasing the friction coefficient [134]. The increased temperature not only accelerates wear by reducing the hardness of the tool material, but also negatively affects the surface integrity of the workpiece (microstructural changes, residual stresses) [135]. From an energy efficiency perspective, there is a direct correlation between tool wear and power consumption [136]. Loss of cutting-edge sharpness increases the specific cutting force required to remove chips. This situation requires the machine spindle to produce more torque, which can increase total power consumption by 20% to 40% [137]. Furthermore, cutting tool wear significantly impacts production efficiency and costs [138]. Consequently, tool wear is not merely a physical loss of material but a multi-parameter process that affects the entire value chain, from surface quality to energy consumption, production speed, and final cost. For all these reasons, this section of the study examines the wear process and behavior of cutting tools under different cooling applications and aims to provide recommendations to delay wear. Two different procedures were carried out during the investigation of tool wear. First, a microscope was used to quantify flank wear; the results are shown graphically in Fig. 14. Using a new cutting edge, a chip-removal process with a fixed volume of 6000 mm^3 was applied for each cooling condition. During chip removal, the extent of wear was measured and recorded at 1500 mm^3 intervals. Thus, the progression of wear at different chip volumes was revealed.

Dry cutting conditions resulted in a maximum flank wear of 377 μ, as seen in Fig. 14. Severe heat accumulation in the cutting zone during cutting superalloys like Inconel X-750, which have limited thermal conductivity and good chemical resistance at high temperatures, explains this expected occurrence. In other words, since the high heat generated during the cutting of nickel-based superalloys cannot be effectively dissipated, adhesion occurs at the tool-chip-workpiece interface, leading to built-up edge (BUE) formation. Upon initiation of BUE, the chip adheres to the cutting tool, eventually leading to periodic fragmentation. The microcracks and surface damage resulting from these fractures cause rapid flank wear [139]. Additionally, the hard phases and carbide-based abrasives inherent in the microstructure of nickel-based superalloys exert mechanical abrasion during contact, leading to rapid degradation and elevated flank wear [133]. With the integration of multiple cooling methods into the system, various reductions in flank wear were observed. In terms of proportional reductions compared to dry machining, the flank wear decreased by 23.61% for vortex, 37.67% for pure MQL, and 47.21% for pure MQL+vortex.

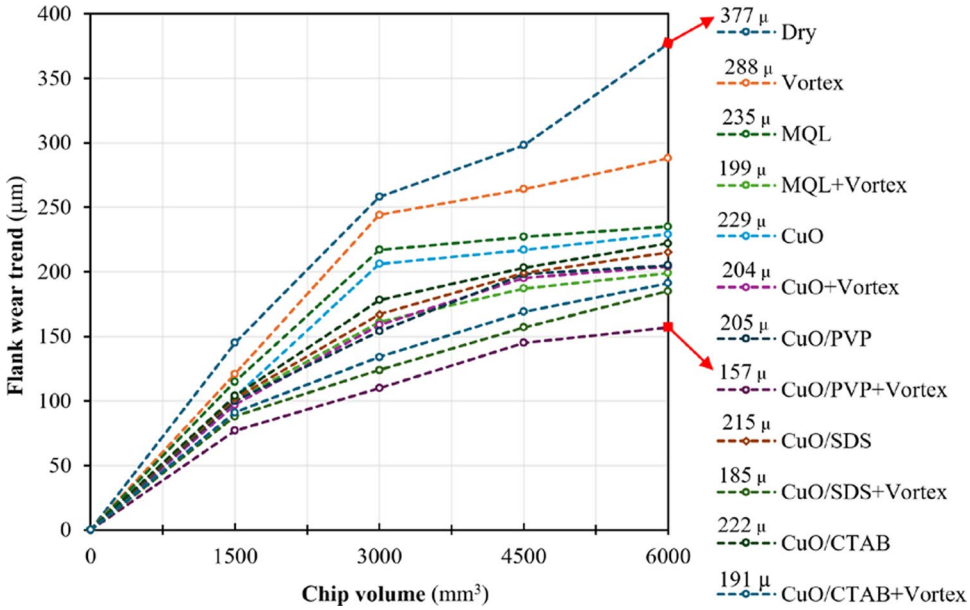

Fig. 14 Flank wear trends under different cooling/lubrication environments (after 6000 mm^3 chip volume)

Furthermore, reductions were recorded at 39.25% for CuO-doped nanofluid, 45.89% for CuO+vortex, 45.62% for PVP-surfactant added CuO, and a maximum of 58.36% for CuO/PVP+vortex. Similarly, the values for SDS-added CuO, CuO/SDS+vortex, CTAB-added CuO, and CuO/CTAB+vortex were 42.97%, 50.93%, 41.11%, and 49.34%, respectively. According to the results presented in Sect. 3.1, PVP exhibits superior nanoparticle stability, wettability, and tribological film-forming capability compared to the other surfactants used. Furthermore, its thermal conductivity is better than that of other surfactants. It is thought that PVP creates a more effective surface film by ensuring the homogeneous distribution of CuO nanoparticles within the nanofluid and maintaining their stability over a long period. Consequently, the formation of a tribofilm at the tool-workpiece-chip interfaces becomes more effective, thereby reducing the friction and wear energy [140]. This situation is also consistent with the cutting temperature results presented in Sect. 3.2. Additionally, faster heat dissipation from the cutting zone is ensured by the integrated usage of a vortex tube. Thus, the effects of adhesive wear and thermal softening are significantly mitigated, leading to an improvement in flank wear values [29].

In the second stage of this section, the wear mechanisms that led to the cutting tool's breakdown were identified using SEM and EDX analyses. An examination of Figs. 15, 16, and 17 reveal that tool failure results from the combined effects of mechanisms such as adhesion, abrasion, diffusion, and thermomechanical fatigue, rather than a single dominant mechanism. Significant crater wear on the rake face, considerable built-up edge (BUE) and built-up layer (BUL) production, microcracks, coating delamination, and edge chipping were all noted when the wear processes under dry cutting circumstances were investigated (Fig. 15). Ni, Fe, and Cr elements were found as a consequence of the EDX study done on the wear zones (Tables 2, 3, and 4). This circumstance suggests that adhesive wear is evident and that there is transfer of material from the workpiece to the cutting tool. The heat generated during machining concentrates at the tool-chip-workpiece interface because nickel-based superalloys exhibit limited thermal conductivity and high-temperature resistance [141, 142]. The high temperature at the tool-chip-workpiece interface accelerates crater wear due to diffusion at the cutting edge. The cobalt in the cutting tool and the Ni-based workpiece migrate elements, causing the tool coating to delaminate and the substrate to become exposed. Akthar et al. [143] reported that during cutting of nickel-based superalloys, the tool material loses strength due to excessive heating, and diffusion and chemical wear become active, thereby increasing the tool wear rate. A similar situation occurred here, and the cutting process conducted under dry processing conditions generated excessive heat, triggering diffusion wear. As the protective properties of the cutting tool coating deteriorated, adhesive interactions increased, and local stress concentrations formed at the cutting edge. The periodic entry and exit of the cutting edge into the material, specific to the milling process, induce thermal cycles and microcrack formation due to thermomechanical fatigue [144]. This explains the cause of fatigue-induced edge fractures. Another type of wear observed in cutting tools is flank wear. Flank wear occurring in cutting tools is thought to be caused by the combined effect of abrasion and adhesion. It is observed that the precipitates of Inconel X-750 and the surface layer that hardens during cutting produce abrasion marks parallel to the cutting direction on the cutting tool surface. This wear

Table 2 EDX analysis of worn cutting tool under different nanofluid environments (from Fig. 15 EDX spots)

EDX No.	C%	O%	Al%	Cr%	Mn%	Fe%	Co%	Ni%	Rb%	W%	N%	Ti%	Sr%	Ba%	Cu%
1	5.4	0.6	0.4	1.8	0.1	0.9	8.7	3.8	1	77.3	–	–	–	–	–
2	16.5	8.8	20	2.9	–	1.7	–	14.6	–	–	20.8	14.7	–	–	–
3	15.5	–	0.9	9.5	–	4.3	1.6	41.5	–	22.5	–	0.9	1.1	2.3	–
4	9.5	1.6	1.3	13.9	0.5	6.4	–	64.8	–	–	–	2.1	–	–	–
5	7.4	9.5	24.8	2.6	–	1.8	–	11.3	–	–	22.2	20.3	–	–	–
6	7.9	2.3	–	2.4	0.2	0.9	3.6	6	–	76.8	–	–	–	–	–
7	13.5	5.6	1	9.9	–	5.2	5	51.9	–	–	–	2.6	–	–	15.2
8	9.6	6.2	24.1	1.5	–	–	–	2.9	–	7.1	28.4	20.2	–	–	–
9	60.4	5.4	–	5.2	–	2.5	–	20.8	–	–	–	1.2	–	–	4.5
10	14.1	2.7	–	2.3	–	1.6	6.4	11.7	2.2	59.1	–	–	–	–	–
11	–	5.7	32	0.7	–	–	1.1	1.6	–	–	34.8	24.1	–	–	–
12	14.8	1.2	0.8	13.5	0.3	6.6	–	60.2	–	–	–	1.8	–	0.7	–

condition arises from the hard, abrasive carbides present in nickel-based superalloys. Liang et al. [145] reported that the high heat and high pressure generated during the cutting of Ni-based superalloys exacerbate severe friction and extrusion. In addition, the repeated formation, growth, and breakage of BUE caused material to break off from the cutting tool, thereby accelerating flank wear. The process, which began with micro-chipping in the initial stage, progressed to the fracture stage. Another situation shown in Fig. 15 is a cutting operation in which the vortex tube and MQL system are used separately or together. Using the vortex system, the tendency toward diffusion has decreased, but micro-BUL has persisted. The decrease in diffusion tendency is associated with vortex-induced cooling, while the persistence of micro-BUL is associated with insufficient lubrication. In hybrid cooling, where the vortex and MQL systems are used together, both cooling and lubrication can be achieved to some extent, thereby reducing flank wear. When nanofluids are used, wear mechanisms are much improved (Figs. 16 and 17). The use of nanoparticles has been credited with improving the base fluid's tribological and thermal characteristics. The use of nanoparticles increases thermal conductivity in the base fluid and effectively dissipates heat in the cutting zone [146]. Furthermore, nanoparticles that enter the tool-chip-workpiece interface form a protective tribofilm, reducing friction [147]. In addition, CuO nanoparticles with a globular morphology exhibit a “rolling effect” mechanism, thereby reducing shear stress [148]. This may also be one of the main factors in reducing wear. It is thought that nanofluids stabilized by adding surfactants to CuO-containing nanofluids exhibit a more homogeneous distribution and thus reduce wear. In the hybrid cooling method, where CuO+surfactant-enhanced nanofluids are used in conjunction with vortex, both cooling and lubrication are utilized in an advanced manner, effectively controlling wear mechanisms. Thus, the structural integrity of the cutting edge is preserved for a longer period. As a result, tool wear during the machining of Inconel X-750 begins with adhesive effects and continues with abrasive flank wear, driven by diffusion-based crater wear. Subsequently, thermomechanically induced microcracks form and the process continues until fracture. The SEM photographs and EDX analyses presented in this study clearly demonstrate that adhesive wear is the primary mechanism, while temperature and thermal cycles accelerate fracture. By reducing temperature and friction at the tool-chip-workpiece interface, the cooling techniques employed during machining greatly reduce the severity of these wear processes.

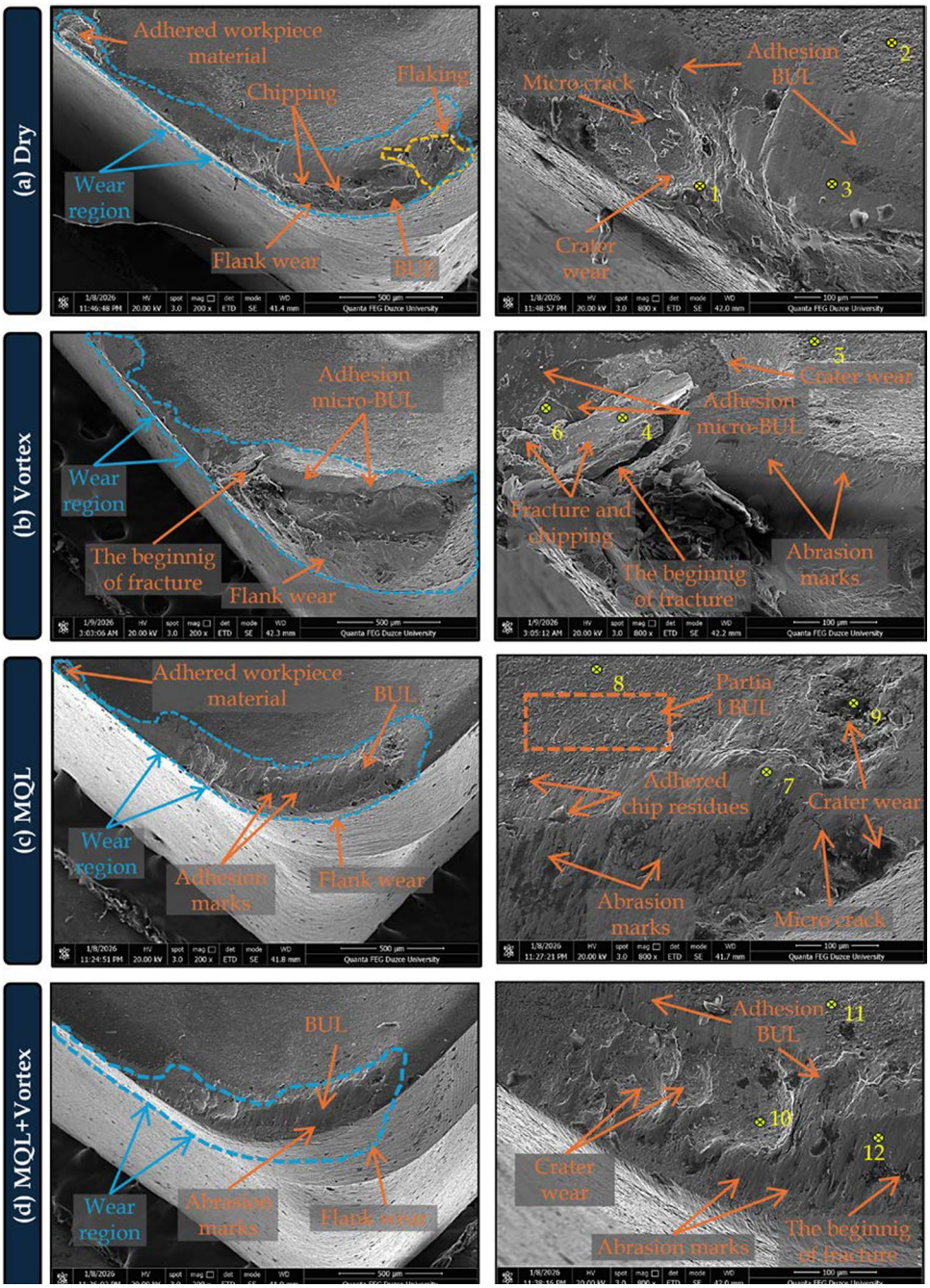

Fig. 15 SEM images of worn cutting tool under; **a** dry, **b** Vortex, **c** MQL, and **d** MQL+Vortex

4 Conclusion

This study investigated the machining of Inconel X-750 alloy using an eco-friendly process that combines vortex-based cryogenic cooling with Minimum Quantity Lubrication (MQL) employing surfactant-modified CuO nanofluids. Twelve different conditions were evaluated in the experimental study, and machinability characteristics were analyzed alongside fundamental thermomechanical and tribological data. Key findings based on comprehensive comparisons are summarized below:

- The incorporation of CuO nanoparticles significantly increased the thermal conductivity of the base fluid (by up to 201.84%), thereby greatly enhancing heat transfer. Although the addition of surfactants (PVP, SDS, and CTAB) slightly reduced thermal conductivity, it critically altered the fluid's rheology. Changes in kinematic viscosity, pH, and contact angle induced by the surfactants radically transformed droplet dynamics; they ensured colloidal stability and promoted denser, localized fluid retention in the cutting zone rather than rapid atomization.

Table 3 EDX analysis of worn cutting tool under different nanofluid environments (from Fig. 16 EDX spot)

EDX No.	C%	O%	Al%	Cr%	Mn%	Fe%	Co%	Ni%	Rb%	W%	N%	Ti%	Sr%	Ba%	Cu%
1	11	1.9	–	1.1	–	–	1.9	2.2	–	81.8	–	–	–	–	–
2	10.7	–	26.3	–	–	–	–	–	–	9.8	32.5	20.7	–	–	–
3	11.6	2.7	0.8	13.7	0.2	6.6	–	59.4	–	–	–	1.8	–	1	2.3
4	9.6	2.2	–	1.7	–	–	2.8	–	–	83.7	–	–	–	–	–
5	16	3.8	22.9	–	–	–	–	–	–	11.1	29	17.2	–	–	–
6	17.5	2.5	–	12.4	–	6.5	–	54.6	–	–	–	1.6	–	–	4.9
7	15.3	2.2	–	1.8	–	0.8	3.1	1.5	–	75.3	–	–	–	–	–
8	10.4	6.9	24.7	2.2	–	1.9	–	9.6	–	–	21.1	23.3	–	–	–
9	17.1	1.2	0.9	12.6	0.3	6.7	–	58.5	–	–	–	1.8	–	–	0.9
10	25.2	2.5	–	–	–	1.1	2.9	1.8	–	66.5	–	–	–	–	–
11	14.7	4.7	23.3	–	–	–	–	–	–	9.3	30	18.1	–	–	–
12	15.6	3.8	1.9	9.7	0.3	5.6	–	44.6	–	–	–	0.9	–	2.4	15.3

Table 4 EDX analysis of worn cutting tool under different nanofluid environments (from Fig. 17 EDX spot)

EDX No.	C%	O%	Al%	Cr%	Mn%	Fe%	Co%	Ni%	Rb%	W%	N%	Ti%	Sr%	Ba%	Cu%
1	14.6	2.6	–	1.5	–	–	3.5	2.2	–	75.5	–	–	–	–	–
2	12	–	28.3	–	–	–	–	22.9	–	–	36.8	–	–	–	–
3	20.2	1.5	0.8	12.9	–	6.1	–	55.9	–	–	–	1.9	–	–	0.7
4	26.5	3.3	–	2.8	–	–	15.6	2.3	–	49.5	–	–	–	–	–
5	18.2	6.9	22.6	–	–	–	–	7.4	–	–	25.3	19.7	–	–	–
6	18	2.9	1.1	12.1	–	6.1	–	54.9	–	–	–	2.3	–	–	2.6
7	14.2	2.8	–	2.3	–	1.1	3.1	3.2	–	73.2	–	–	–	–	–
8	16.3	9.9	24.5	–	–	1.1	–	1.6	–	–	25.8	20.8	–	–	–
9	13.7	0.9	2.3	11.7	–	5.9	–	57.8	–	–	–	–	–	–	5.8
10	17.2	4	0.8	3.2	–	1.6	1.9	4.7	–	65.3	–	1.4	–	–	–
11	25.3	13.3	16.5	2.2	–	3.3	–	5.8	–	–	7.6	15.2	–	–	10.7
12	16.7	–	2.8	10.7	–	6.3	–	52.4	–	–	5.9	5.3	–	–	–

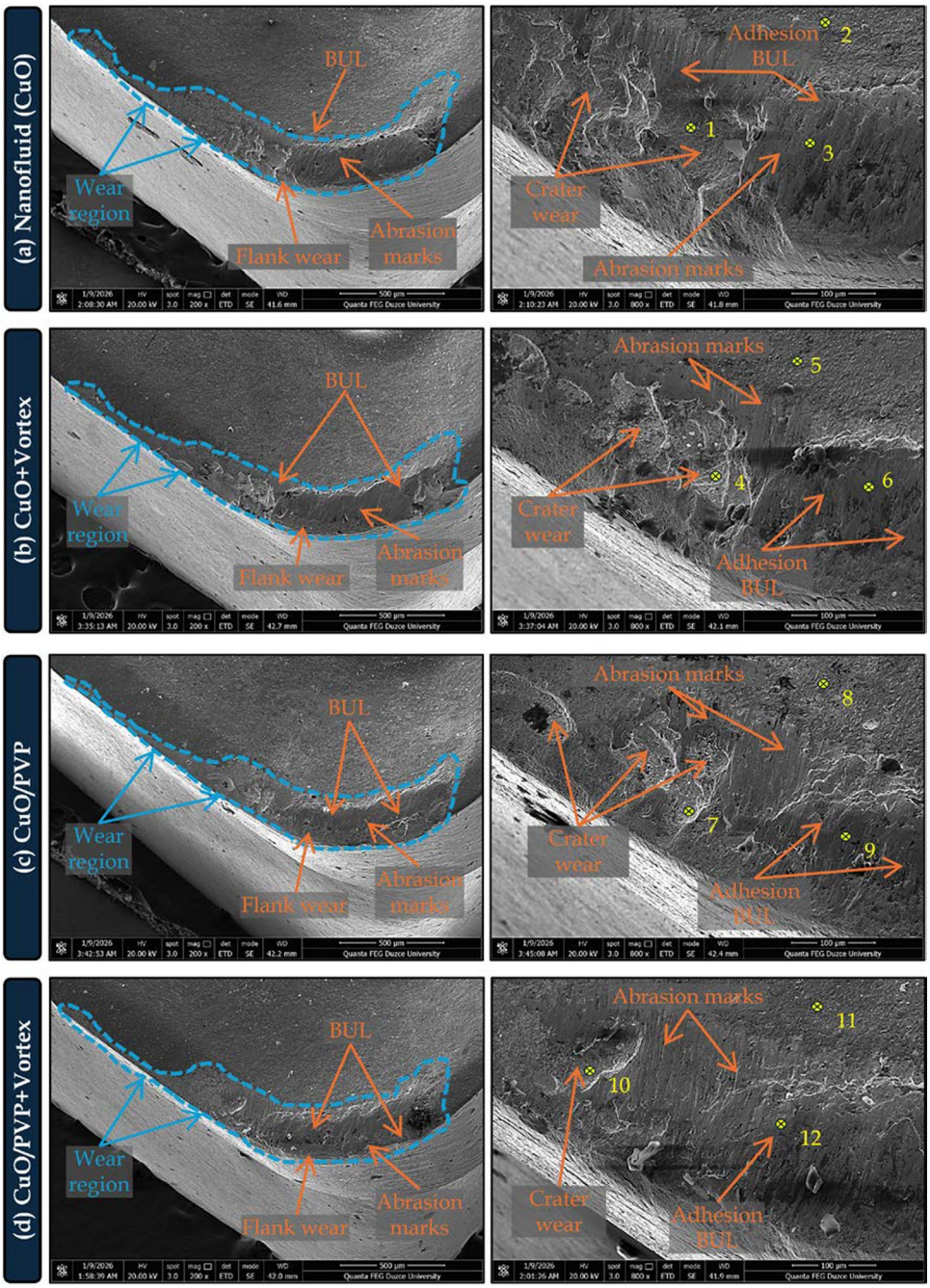

Fig. 16 SEM images of worn cutting tool under; **a** CuO, **b** CuO+Vortex, **c** CuO/PVP, and **d** CuO/PVP+Vortex

- The hybrid application of vortex cooling and nanofluid lubrication at sub-zero temperatures significantly altered thermodynamic interactions at the tool-chip interface. Effective cooling and fluid penetration resulted in superior tribological performance at the tool-chip-workpiece interfaces. Consequently, temperatures in the cutting zone were optimized. The sterically stabilized CuO/PVP+vortex cooling configuration provided the best thermal management, reducing the cutting temperature by 37.77% (from 323 °C to 201 °C) compared to dry cutting.
- The superior mechanisms exhibited by the surfactant-modified CuO nanoparticles-namely polishing, rolling, sliding, and mending-facilitated the formation of a durable, wear-reducing tribofilm. This mechanical lubrication effect minimized plastic deformation and shear stress, resulting in a significant reduction in power consumption (up to 25%). Furthermore, this protective film enabled the CuO/PVP+vortex strategy to reduce average surface roughness (Ra) by 64.04% and improve surface quality from 0.470 µm to an impressive 0.169 µm.

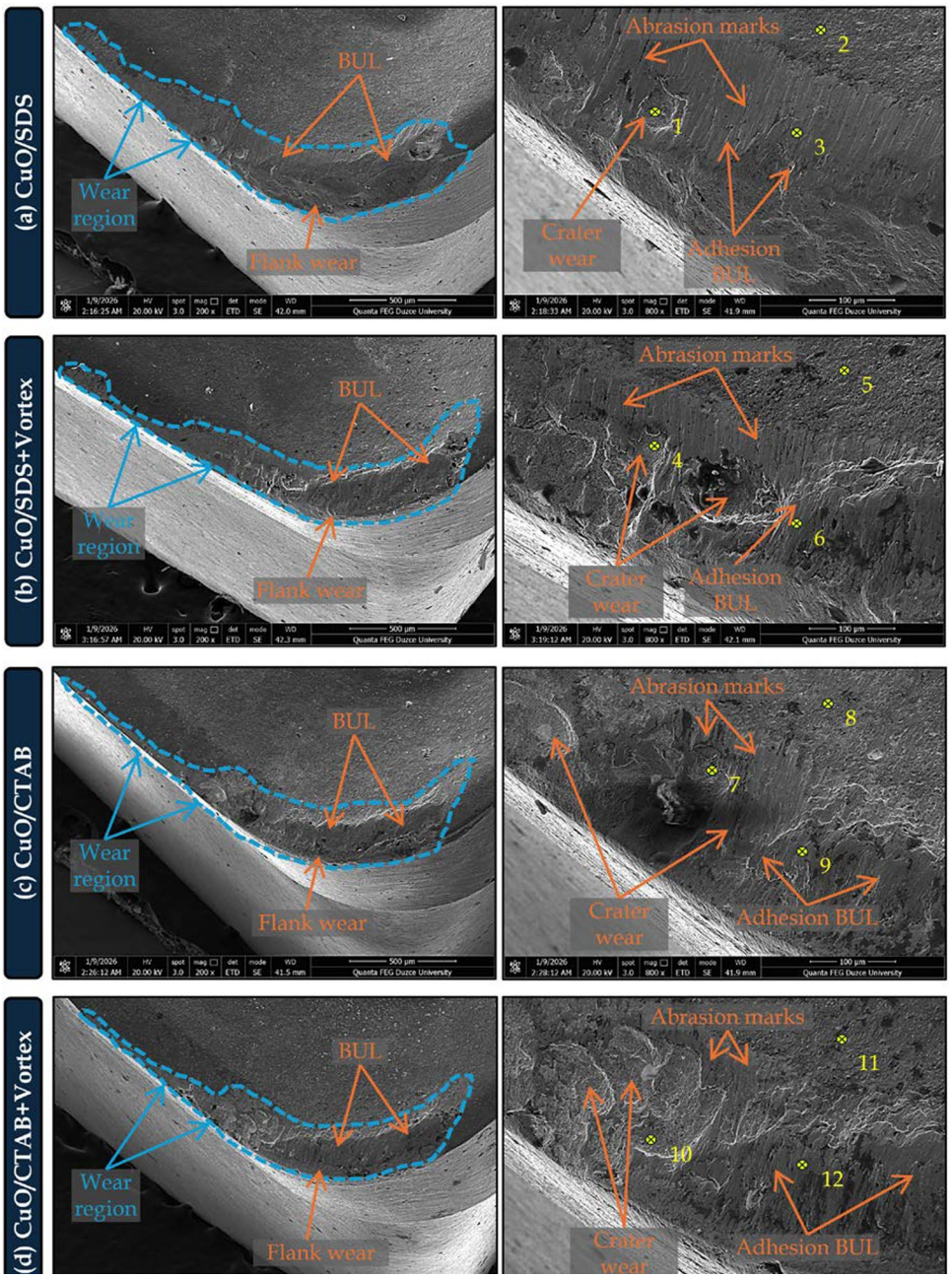

Fig. 17 SEM images of worn cutting tool under; **a** CuO/SDS, **b** CuO/SDS+Vortex, **c** CuO/CTAB, and **d** CuO/CTAB+Vortex

- During dry cutting, severe thermomechanical loads-combined with adhesion, abrasive wear, diffusion, and rapidly forming Built-Up Edge (BUE) and Built-Up Layer (BUL) led to rapid tool degradation, resulting in 377 µm of flank wear. However, the synergistic protection provided by the combination of nano-lubrication and vortex cooling-which maintained tool rigidity, significantly mitigated these wear mechanisms. The superior effectiveness of the CuO/PVP+vortex approach preserved cutting edge integrity, reduced flank wear by 58.36% (bringing it down to 157 µm), and significantly extended tool life.

In summary, the combination of non-ionic PVP-modified CuO nanofluid lubrication and vortex tube cooling has emerged as the optimal strategy in terms of thermomechanical and tribological performance. Thanks to this highly synergistic hybrid setup, the proposed method is expected to contribute significantly to the clean machining efficiency required in critical sectors such as the aerospace and advanced metalworking industries.

Acknowledgements The authors acknowledge with thanks the Erciyes University (Türkiye) Research Fund for financial support of this study (Project No: FYL-2024-14148).

Author contributions Cemal Şimşek: Methodology, Writing – original draft, Investigation, Data curation. Çağrı Vakkas Yıldırım: Writing – review & editing, Software, Resources, Methodology, Supervision. Şenol Şirin: Investigation, Writing – original draft, Validation, Visualization, Methodology.

Funding This study was funded by Erciyes University (Türkiye) Research Fund (Project No: FYL-2024-14148).

Data availability The data that support the findings of this study are available from the corresponding author upon reasonable request.

Declarations

Conflict of interest The authors declare that they have no known competing financial interests or personal relationships that could have appeared to influence the work reported in this paper.

References

1. Stephens JR (1987) Superalloy resources: supply and availability. NASA Tech Memo 1987;89866
2. Pollock TM, Tin S (2012) Nickel-based superalloys for advanced turbine engines: chemistry, microstructure and properties. J Propul Power 22:361–374. https://doi.org/10.2514/1.18239
3. Perrut M, Caron P, Thomas M, Couret A (2018) High temperature materials for aerospace applications: Ni-based superalloys and γ-TiAl alloys. C R Phys 19:657–671. https://doi.org/10.1016/j.crhy.2018.10.002
4. Schulz F, Lindgren K, Xu J, Hryha E (2024) Gamma prime formation in nickel-based superalloy IN738LC manufactured by laser powder bed fusion. Mater Today Commun 38:107905. https://doi.org/10.1016/j.mtcomm.2023.107905
5. Li Z, Wang Z, Wang Z, Qin Z, Liu F, Tan L et al (2023) Quantifying solid solution strengthening in nickel-based superalloys via high-throughput experiment and machine learning. Comput Model Eng Sci 135:1521–1538. https://doi.org/10.32604/cmes.2022.021639
6. Gong N, Meng TL, Teo SL, Cao J, Lee CJJ, Tan CKI et al (2023) High-temperature oxidation and hot corrosion of Ni-based single crystal superalloy in the incubation stage. Corros Sci 214:111026. https://doi.org/10.1016/j.corsci.2023.111026
7. Rahman M, Seah WKH, Teo TT (1997) The machinability of inconel 718. J Mater Process Technol 63:199–204. https://doi.org/10.1016/S0924-0136(96)02624-6
8. Thellaputta GR, Chandra PS, Rao CSP (2017) Machinability of nickel based superalloys: a review. Mater Today Proc 4:3712–3721. https://doi.org/10.1016/j.matpr.2017.02.266
9. Choudhury IA, El-Baradie MA (1998) Machinability of nickel-base super alloys: a general review. J Mater Process Technol 77:278–284. https://doi.org/10.1016/S0924-0136(97)00429-9
10. Polo S, Rubio EM, Marín MM, Sáenz de Pipaón JM (2025) Evolution and latest trends in cooling and lubrication techniques for sustainable machining: a systematic review. Processes. https://doi.org/10.3390/pr13020422
11. Kui GWA, Islam S, Reddy MM, Khandoker N, Chen VLC (2021) Recent progress and evolution of coolant usages in conventional machining methods: a comprehensive review. Int J Adv Manuf Technol 119(1):3–40. https://doi.org/10.1007/s00170-021-08182-0
12. Jayal AD, Balaji AK (2009) Effects of cutting fluid application on tool wear in machining: interactions with tool-coatings and tool surface features. Wear 267:1723–1730. https://doi.org/10.1016/j.wear.2009.06.032
13. Said Z, Gupta M, Hegab H, Arora N, Khan AM, Jamil M et al (2019) A comprehensive review on minimum quantity lubrication (MQL) in machining processes using nano-cutting fluids. Int J Adv Manuf Technol 105:2057–2086. https://doi.org/10.1007/s00170-019-04382-x
14. Liu H, Meurer M, Schraknepper D, Bergs T (2022) Investigation of the cutting fluid's flow and its thermomechanical effect on the cutting zone based on fluid–structure interaction (FSI) simulation. Int J Adv Manuf Technol 121(1):267–281. https://doi.org/10.1007/s00170-022-09266-1
15. Khan MAA, Hussain M, Lodhi SK, Zazoum B, Asad M, Afzal A (2022) Green metalworking fluids for sustainable machining operations and other sustainable systems: a review. Metals. https://doi.org/10.3390/met12091466
16. Schwarz M, Dado M, Hnilica R, Veverková D. Environmental and Health Aspects of Metalworking Fluid Use. Pol J Environ Stud 2015;24.
17. Wickramasinghe KC, Sasahara H, Rahim EA, Perera GIP (2020) Green metalworking fluids for sustainable machining applications: a review. J Clean Prod 257:120552. https://doi.org/10.1016/j.jclepro.2020.120552
18. Calvert GM, Ward E, Schnorr TM, Fine LJ (1998) Cancer Risks Among Workers Exposed to Metalworking Fluids: A Systematic Review. J Ind Med 33:282–292. https://doi.org/10.1002/(SICI)1097-0274(199803)33:3%3c282::AID-AJIM10%3e3.0.CO;2-W
19. Cheng C, Phipps D, Alkhaddar RM (2005) Treatment of spent metalworking fluids. Water Res 39:4051–4063. https://doi.org/10.1016/j.watres.2005.07.012
20. Liu H, Meurer M, Bergs T (2024) Effect of cutting fluid supply conditions on tool loads during continuous and interrupted orthogonal cutting. Int J Adv Manuf Technol 135(11):5141–5155. https://doi.org/10.1007/s00170-024-14683-5
21. Khan AM, Rahat MR, Ahmed U, Jamil M, Ali MA, Zhao G et al (2025) The recent advancements in minimum quantity lubrication (MQL) and its application in mechanical machining—a state-of-the-art review. Lubricants. https://doi.org/10.3390/lubricants13090401
22. Sharma AK, Tiwari AK, Dixit AR (2016) Effects of minimum quantity lubrication (MQL) in machining processes using conventional and nanofluid based cutting fluids: a comprehensive review. J Clean Prod 127:1–18. https://doi.org/10.1016/j.jclepro.2016.03.146
23. Wang Y, Liu C (2023) State-of-the-art on minimum quantity lubrication in green machining. J Clean Prod 429:139613
24. Wu S, Liu G, Zhang W, Chen W, Wang C (2023) High-speed milling of hardened steel under minimal quantity lubrication with liquid nitrogen. J Manuf Process 95:351–368
25. Patra SK, Swain S (2022) Effects of minimum quantity lubrication (MQL) in grinding: principle, applications and recent advancements. Mater Today Proc 69:96–106
26. Bhowmik A, Kumar R, Thulasiram R, Karthikeyan A, Thatoi DN, Bisht YS et al (2025) A comprehensive review on the viability of minimum quantity lubrication technology for machining difficult-to-cut alloys. AIP Adv 15:1. https://doi.org/10.1063/5.0256932
27. Venkatesh R (2024) Surface-treated jute fiber-blended epoxy composite featured with SiC via injection molding process: characteristics study. J Inst Eng. https://doi.org/10.1007/s40033-024-00722-8
28. Venkatesh R. Development and Behavior Analysis of CNT Fibers Reinforced High-Density Polyethylene Composite via Compression Mold Route. Journal of The Institution of Engineers (India): Series D 2024. https://doi.org/10.1007/s40033-024-00718-4.
29. Amin AR, Ali A, Ali HM, Amin AR, Ali A, Ali HM (2022) Application of nanofluids for machining processes: a comprehensive

review. Nanomaterials (Basel). https://doi.org/10.3390/NANO12234214
30. Yıldırım ÇV, Sarıkaya M, Kıvak T, Şirin Ş (2019) The effect of addition of hBN nanoparticles to nanofluid-MQL on tool wear patterns, tool life, roughness and temperature in turning of Ni-based Inconel 625. Tribol Int 134:443–456. https://doi.org/10.1016/j.triboint.2019.02.027
31. Şirin E, Yıldırım ÇV, Şirin Ş, Kıvak T, Sarıkaya M (2024) Comprehensive analysis of cutting temperature, tool wear, surface integrity and tribological properties in sustainable milling of Ti6Al4V alloy: LN2, nanofluid and hybrid machining. J Manuf Process 131:1360–1371
32. Korkmaz ME, Gupta MK (2024) Nano lubricants in machining and tribology applications: a state of the art review on challenges and future trend. J Mol Liq 407:125261
33. Venkatesh R (2026) Effect of hybrid nanofluid and polyethylene glycol/aluminium foam on thermal characteristics and energy storage performance of solar air heater. Appl Therm Eng. https://doi.org/10.1016/j.applthermaleng.2026.130213
34. Fernando R, Wickramasinghe KC, Sasahara H (2025) Nanoparticles for the prominent tribological and rheological properties of greener metalworking fluids–a review. J Mol Liq. https://doi.org/10.1016/j.molliq.2025.128513
35. Hu S, Li C, Zhou Z, Liu B, Zhang Y, Yang M et al (2023) Nanoparticle-enhanced coolants in machining: mechanism, application, and prospects. Front Mech Eng 18(4):53. https://doi.org/10.1007/s11465-023-0769-8
36. Bacha HB, Ullah N, Hamid A, Shah NA (2024) A comprehensive review on nanofluids: synthesis, cutting-edge applications, and future prospects. Int J Thermofluids 22:100595. https://doi.org/10.1016/j.ijft.2024.100595
37. Wang J, Yang X, Klemeš JJ, Tian K, Ma T, Sunden B (2023) A review on nanofluid stability: preparation and application. Renew Sustain Energy Rev 188:113854. https://doi.org/10.1016/J.RSER.2023.113854
38. Chakraborty S, Panigrahi PK (2020) Stability of nanofluid: a review. Appl Therm Eng 174:115259. https://doi.org/10.1016/j.applthermaleng.2020.115259
39. Mahbubul IM, Elcioglu EB, Saidur R, Amalina MA (2017) Optimization of ultrasonication period for better dispersion and stability of TiO2–water nanofluid. Ultrason Sonochem 37:360–367
40. Xian HW, Sidik NAC, Saidur R (2020) Impact of different surfactants and ultrasonication time on the stability and thermophysical properties of hybrid nanofluids. Int Commun Heat Mass Transfer 110:104389
41. Farade RA, Wahab NIA, Said Z, Khan TMY, Saleel CA (2025) Toward green and sustainable dielectric nanofluids: surfactant impacts on stability, properties, and regulations. Adv Colloid Interface Sci. https://doi.org/10.1016/j.cis.2025.103668
42. Yıldırım ÇV, Şirin Ş, Kıvak T, Sarıkaya M (2023) The effect of nanofluids reinforced with different surfactants on the machining and friction-wear properties of Waspaloy. Tribol Int 181:108316
43. Abellán-Nebot JV, Ameen KH, Khan AM, Mondragón R (2024) Application of hybrid nanofluids in MQL assisted machining operations: exploring synergies and establishing guidelines. Int J Precis Eng Manuf-Green Technol 12(2):657–689. https://doi.org/10.1007/s40684-024-00675-z
44. Dennison MS, Jebabalan SK, Barik D (2024) Applicability of nano-cutting fluids for enhanced cooling, low tool wear, and high tribological performance during machining—a review. Discov Appl Sci 6(12):663-. https://doi.org/10.1007/s42452-024-06398-9
45. Manikanta JE, Abdullah M, Ambhore N, Kotteda TK (2025) Analysis of machining performance in turning with trihybrid nanofluids and minimum quantity lubrication. Sci Rep 15(1):12194-. https://doi.org/10.1038/s41598-025-97039-7
46. Swain S, Patra SK, Roul MK, Sahoo LK (2022) A short review on cooling process using compressed cold air by vortex tube in machining. Mater Today Proc 64:382–389
47. Subudhi S, Sen M (2015) Review of Ranque–Hilsch vortex tube experiments using air. Renew Sustain Energy Rev 52:172–178
48. Celent L, Bajić D, Jozić S, Mladineo M (2023) Hard milling process based on compressed cold air-cooling using vortex tube for sustainable and smart manufacturing. Machines. https://doi.org/10.3390/machines11020264
49. Mahapatro K, Krishna PV (2022) Influence of flow parameters in the dual nozzle CO2-based vortex tube cooling system during turning of Ti-6Al-4V. Proc Inst Mech Eng C J Mech Eng Sci 236:4828–4842. https://doi.org/10.1177/09544062211057495
50. Alsayyed B, Hamdan MO, Aldajah S (2013) Vortex Tube Impact on Cooling Milling Machining. ASME Int Mech Eng Congr Expo, Proc 3:773–6. https://doi.org/10.1115/IMECE2012-89885
51. Taha Z, Salaam HA, Tuan Ya TMYS, Phoon SY, Tan CF, Akiah MA (2013) Vortex tube air cooling: the effect on surface roughness and power consumption in dry turning. Int J Automot Mech Eng 8:1477–1586. https://doi.org/10.15282/ijame.8.2013.34.0122
52. Valić GŠ, Kostadin T, Cukor G, Fabić M, Valić GŠ, Kostadin T et al (2023) Sustainable machining: MQL technique combined with the vortex tube cooling when turning martensitic stainless steel X20Cr13. Machines. https://doi.org/10.3390/MACHINES11030336
53. Khalil ANM, Azmi AI, Murad MN, Annuar AF, Ali MAM (2019) Coupled effects of vortex tube hybrid cooling with minimal quantity reinforced nanoparticle lubricants in turning NiTi alloys. Int J Adv Manuf Technol 105:3007–3015. https://doi.org/10.1007/S00170-019-04507-2/FIGURES/6
54. Singh GR, Sharma VS (2016) Analyzing machining parameters for commercially puretitanium (Grade 2), cooled using minimum quantity lubrication assisted by a Ranque-Hilsch vortex tube. Int J Adv Manuf Technol 88(9):2921–2928. https://doi.org/10.1007/s00170-016-8982-9
55. Singh G, Pruncu CI, Gupta MK, Mia M, Khan AM, Jamil M et al (2019) Investigations of machining characteristics in the upgraded MQL-assisted turning of pure titanium alloys using evolutionary algorithms. Materials (Basel). https://doi.org/10.3390/ma12060999
56. Ayhan MÖ, Şirin E, Yildirim ÇV (2024) The effect of environmentally friendly cooling techniques in hard turning: comparison of nanofluid, vortex, GQDs and hybrid cooling methods. Arab J Sci Eng 50(22):18469–18490. https://doi.org/10.1007/s13369-024-09795-9
57. Şirin Ş, Kıvak T (2019) Performances of different eco-friendly nanofluid lubricants in the milling of Inconel X-750 superalloy. Tribol Int 137:180–192. https://doi.org/10.1016/j.triboint.2019.04.042
58. Khatai S, Sahoo AK, Kumar R, Panda A (2025) Investigation on machinability and sustainability aspects during hard turning under GO nanofluid MQL environment for precision and cleaner manufacturing. Precis Eng 95:379–408. https://doi.org/10.1016/j.precisioneng.2025.05.006
59. Çakır Şencan A (2026) Comparison of the performance of vegetable-based nanofluids enriched with hBN and SiO_2 in the machining of Ti6Al4V alloy under MQL conditions. J Manuf Process 164:377–399. https://doi.org/10.1016/j.jmapro.2026.02.058
60. Xuan Y, Li Q (2000) Heat transfer enhancement of nanofluids. Int J Heat Fluid Flow 21:58–64
61. Indhuja A, Suganthi KS, Manikandan S, Rajan KS (2013) Viscosity and thermal conductivity of dispersions of gum arabic capped MWCNT in water: influence of MWCNT concentration and temperature. J Taiwan Inst Chem Eng 44:474–479

62. Şirin E, Kıvak T, Yıldırım ÇV (2021) Effects of mono/hybrid nanofluid strategies and surfactants on machining performance in the drilling of Hastelloy X. Tribol Int 157:106894
63. Kumar PG, Kumaresan V, Velraj R (2017) Stability, viscosity, thermal conductivity, and electrical conductivity enhancement of multi-walled carbon nanotube nanofluid using gum arabic. Fullerenes Nanotubes Carbon Nanostruct 25:230–240. https://doi.org/10.1080/1536383X.2017.1283615
64. Keller BP, Nelson SE, Walton KL, Ghosh TK, Tompson RV, Loyalka SK (2015) Total hemispherical emissivity of Inconel 718. Nucl Eng Des 287:11–18
65. Raja M, Vijayan R, Dineshkumar P, Venkatesan M (2016) Review on nanofluids characterization, heat transfer characteristics and applications. Renew Sustain Energy Rev 64:163–173
66. Porgar S, Oztop HF, Salehfekr S (2023) A comprehensive review on thermal conductivity and viscosity of nanofluids and their application in heat exchangers. J Mol Liq 386:122213
67. Wang J, Li G, Li T, Zeng M, Sundén B (2020) Effect of various surfactants on stability and thermophysical properties of nanofluids. J Therm Anal Calorim 143(6):4057–4070. https://doi.org/10.1007/S10973-020-09381-9
68. Mehrali M, Sadeghinezhad E, Latibari ST, Kazi SN, Mehrali M, Bin MN, et al. Investigation of thermal conductivity and rheological properties of nanofluids containing graphene nanoplatelets. 2014.
69. Cacua K, Ordoñez F, Zapata C, Herrera B, Pabón E, Buitrago-Sierra R (2019) Surfactant concentration and pH effects on the zeta potential values of alumina nanofluids to inspect stability. Colloids Surf A Physicochem Eng Asp 583:123960. https://doi.org/10.1016/J.COLSURFA.2019.123960
70. Peng C, Shen C, Zheng S, Yang W, Hu H, Liu J et al (2017) Transformation of CuO nanoparticles in the aquatic environment: influence of pH, electrolytes and natural organic matter. Nanomaterials (Basel). https://doi.org/10.3390/NANO7100326
71. Singh RK, Sharma AK, Dixit AR, Mandal A, Tiwari AK (2017) Experimental investigation of thermal conductivity and specific heat of nanoparticles mixed cutting fluids. Mater Today Proc 4:8587–8596. https://doi.org/10.1016/J.MATPR.2017.07.206
72. Jang SP, Choi SUS (2004) Role of Brownian motion in the enhanced thermal conductivity of nanofluids. Appl Phys Lett 84:4316–4318. https://doi.org/10.1063/1.1756684
73. Shukla KN, Koller TM, Rausch MH, Fröba AP (2016) Effective thermal conductivity of nanofluids–a new model taking into consideration Brownian motion. Int J Heat Mass Transf 99:532–540
74. Ahmadi MH, Mirlohi A, Alhuyi Nazari M, Ghasempour R (2018) A review of thermal conductivity of various nanofluids. J Mol Liq 265:181–188. https://doi.org/10.1016/J.MOLLIQ.2018.05.124
75. Li H, Wang L, He Y, Hu Y, Zhu J, Jiang B (2015) Experimental investigation of thermal conductivity and viscosity of ethylene glycol based ZnO nanofluids. Appl Therm Eng 88:363–368. https://doi.org/10.1016/J.APPLTHERMALENG.2014.10.071
76. Zhu D, Wang L, Yu W, Xie H (2018) Intriguingly high thermal conductivity increment for CuO nanowires contained nanofluids with low viscosity. Sci Rep 8(1):5282-. https://doi.org/10.1038/s41598-018-23174-z
77. Ali L, Mariam A, Salamat N, Abdal S, Hussain S (2026) Heat transfer analysis on a stretching cylinder with Williamson hybrid nanofluid: effects of convective boundary conditions, Darcy-Forchheimer resistance, and Cattaneo-Christov heat flux. Discover Nano. https://doi.org/10.1186/s11671-026-04770-9
78. Ali L, Murtaza MG, Akter T, Alam J (2026) The effect of electrical conductivity and magnetization on biomagnetic fluid flow containing magnetic particles past a thin needle using lie group analysis. J Therm Anal Calorim. https://doi.org/10.1007/s10973-026-15493-5
79. Park E, Park HW, Lee J (2015) Synthesis of hierarchical copper oxide composites prepared via electrical explosion of the wire in liquids method. Colloids Surf A Physicochem Eng Asp 482:710–717. https://doi.org/10.1016/J.COLSURFA.2015.07.029
80. Sivakumar A, Alagumurthi N, Senthilvelan T (2014) Experimental investigation in thermal conductivity of CuO and ethylene glycol nanofluid in serpentine shaped microchannel. Int J Eng Sci Technol 6:430
81. Apmann K, Fulmer R, Soto A, Vafaei S, Apmann K, Fulmer R (2021) Thermal conductivity and viscosity: review and optimization of effects of nanoparticles. Mater 14:1–75. https://doi.org/10.3390/MA14051291
82. Lei J, Luo Z, Qing S, Huang X, Li F (2022) Effect of surfactants on the stability, rheological properties, and thermal conductivity of Fe3O4 nanofluids. Powder Technol 399:117197. https://doi.org/10.1016/J.POWTEC.2022.117197
83. Vafaei S, Wen D, Borca-Tasciuc T (2011) Nanofluid surface wettability through asymptotic contact angle. Langmuir 27:2211–2218. https://doi.org/10.1021/LA104254A
84. Hernaiz M, Alonso V, Estellé P, Wu Z, Sundén B, Doretti L et al (2019) The contact angle of nanofluids as thermophysical property. J Colloid Interface Sci 547:393–406. https://doi.org/10.1016/J.JCIS.2019.04.007
85. Chu A, Li C, Zhou Z, Liu B, Zhang Y, Yang M et al (2023) Nanofluids minimal quantity lubrication machining: from mechanisms to application. Lubricants. https://doi.org/10.3390/LUBRICANTS11100422
86. Haghnazari S, Abedini V (2021) Effects of hybrid Al2O3–CuO nanofluids on surface roughness and machining forces during turning AISI 4340. SN Appl Sci 3(2):203-. https://doi.org/10.1007/S42452-020-04088-W
87. Sen B, Mia M, Krolczyk GM, Mandal UK, Mondal SP (2019) Eco-friendly cutting fluids in minimum quantity lubrication assisted machining: a review on the perception of sustainable manufacturing. Int J Precis Eng Manuf-Green Technol 8(1):249–280. https://doi.org/10.1007/S40684-019-00158-6
88. Edachery V, Ravi S, Badiuddin AF, Tomy A, Kailas SV, Suvin PS (2022) Wetting behaviour of a green cutting fluid (GCF); influence of surface roughness and surface energy of AA5052, Ti6Al4V and EN31. Mater Today Proc 62:7605–7609. https://doi.org/10.1016/J.MATPR.2022.04.835
89. Vafaei S, Borca-Tasciuc T, Podowski MZ, Purkayastha A, Ramanath G, Ajayan PM (2006) Effect of nanoparticles on sessile droplet contact angle. Nanotechnology 17:2523–2527. https://doi.org/10.1088/0957-4484/17/10/014
90. Wen Y, Zhang C, Zhu G, Wang J, Taqi AAM, Liang T (2025) Combined effects of nanofluid and surfactant on enhanced oil recovery: an experimental study. ACS Omega 10:52375–52386. https://doi.org/10.1021/ACSOMEGA.5C04102
91. Abukhshim NA, Mativenga PT, Sheikh MA (2006) Heat generation and temperature prediction in metal cutting: a review and implications for high speed machining. Int J Mach Tools Manuf 46:782–800. https://doi.org/10.1016/J.IJMACHTOOLS.2005.07.024
92. Nouari M, List G, Girot F, Coupard D (2003) Experimental analysis and optimisation of tool wear in dry machining of aluminium alloys. Wear 255:1359–1368. https://doi.org/10.1016/S0043-1648(03)00105-4
93. Zhao J, Liu Z, Wang B, Hu J, Wan Y (2021) Tool coating effects on cutting temperature during metal cutting processes: comprehensive review and future research directions. Mech Syst Signal Process 150:107302. https://doi.org/10.1016/J.YMSSP.2020.107302
94. Li B, Zhang S, Du J, Sun Y (2022) State-of-the-art in cutting performance and surface integrity considering tool edge microgeometry in metal cutting process. J Manuf Process 77:380–411. https://doi.org/10.1016/J.JMAPRO.2022.03.037

95. Siyambaş Y, Akdulum A, Çakıroğlu R, Uzun G (2025) Estimation of cutting temperature using machine learning based on signal information received from power analyzer in vortex machining conditions. J Manuf Process 137:100–112. https://doi.org/10.1016/J.JMAPRO.2025.02.004
96. He T, Liu N, Xia H, Wu L, Zhang Y, Li D et al (2023) Progress and trend of minimum quantity lubrication (MQL): a comprehensive review. J Clean Prod 386:135809. https://doi.org/10.1016/J.JCLEPRO.2022.135809
97. Arunachalam R, Mannan MA (2000) Machinability of nickel-based high temperature alloys. Mach Sci Technol 4:127–168. https://doi.org/10.1080/10940340008945703;WGROUP:STRING:PUBLICATION
98. Chen H, Liu N, Lu H, Li X, Zheng Y (2024) Evaluation of new nano-cutting fluids for the processing of carbon fiber-reinforced composite materials. J Clean Prod 437:140771. https://doi.org/10.1016/J.JCLEPRO.2024.140771
99. Keklikcioglu Cakmak N (2019) The impact of surfactants on the stability and thermal conductivity of graphene oxide de-ionized water nanofluids. J Therm Anal Calorim 139(3):1895–1902. https://doi.org/10.1007/S10973-019-09096-6
100. Sajid MU, Bicer Y (2022) Impacts of ultrasonication time and surfactants on stability and optical properties of CuO, Fe_3O_4, and CNTs/water nanofluids for spectrum selective applications. Ultrason Sonochem 88:106079. https://doi.org/10.1016/J.ULTSONCH.2022.106079
101. Rehman A, Yaqub S, Ali M, Nazir H, Shahzad N, Shakir S et al (2023) Effect of surfactants on the stability and thermophysical properties of Al_2O_3+TiO_2 hybrid nanofluids. J Mol Liq 391:123350. https://doi.org/10.1016/J.MOLLIQ.2023.123350
102. Manimaran M, Norizan MN, Kassim MHM, Adam MR, Abdullah N, Norrrahim MNF (2025) Critical review on the stability and thermal conductivity of water-based hybrid nanofluids for heat transfer applications. RSC Adv 15:14088–14125. https://doi.org/10.1039/D5RA00844A
103. Yin Q, Gong W, Yang R, Liu S, Xu J, Chen J (2026) Enhancing sustainable machining of Inconel 718 via synergistic coupling of Rehbinder effect and heat transfer using active thermal conductive medium. Materials (Basel). https://doi.org/10.3390/ma19142960
104. Yu Pimenov D, Kiran M, Khanna N, Pintaude G, Cardozo Vasco M, Rosa Ribeiro da Silva L et al (2023) Review of improvement of machinability and surface integrity in machining on aluminum alloys. Int J Adv Manuf Technol 129(11):4743–4779. https://doi.org/10.1007/S00170-023-12630-4
105. Yousefi S, Zohoor M (2019) Effect of cutting parameters on the dimensional accuracy and surface finish in the hard turning of MDN250 steel with cubic boron nitride tool, for developing a knowledged base expert system. Int J Mech Mater Eng 14(1):1. https://doi.org/10.1186/S40712-018-0097-7
106. Pan S, Zhao B, Balaji AK, Qu Y, Yin Y (2024) Perspective: revisiting surface roughness in electrochemical machining and the paradoxes. Surf Sci Technol 2(1):15. https://doi.org/10.1007/S44251-024-00047-4
107. Lu J, Mu H, Ouyang H, Zhang Z, Ding W (2025) Modeling and effect analysis of machining parameters for surface roughness and specific energy consumption during TC18 machining using deep reinforcement learning and neural networks. Artif Intell Rev 58(7):193. https://doi.org/10.1007/S10462-025-11178-X
108. Ruzova TA, Haddadi B (2025) Surface roughness and its measurement methods-analytical review. Results Surf Interfaces. https://doi.org/10.1016/j.rsurfi.2025.100441
109. Venkatesh R (2024) Magnesium alloy and silicon nitrides composite study: synthesis and abrasive water jet machining behavior and optimization. SAE Int J Mater Manuf. https://doi.org/10.4271/05-18-02-0014
110. Isakson S, Sadik MI, Malakizadi A, Krajnik P (2018) Effect of cryogenic cooling and tool wear on surface integrity of turned Ti-6Al-4V. Procedia CIRP 71:254–259. https://doi.org/10.1016/J.PROCIR.2018.05.061
111. Habibnia M, Sheikholeslami M, Tabarhoseini SM, Taheri A, Sheykhi M (2023) Cooling improvement for the machining process with the inclusion of nanoparticles using the experimental approach. J Mol Liq 370:120985. https://doi.org/10.1016/J.MOLLIQ.2022.120985
112. Balasuadhakar A, Kumaran ST, Kurniawan R, Ahmed F (2022) A COMPREHENSIVE REVIEW ON MINIMUM QUANTITY LUBRICATION IN TURNING PROCESS. Surface Rev Lett 29:1. https://doi.org/10.1142/S0218625X22300088
113. Danish M, Aslantas K, Hascelik A, Rubaiee S, Gupta MK, Yildirim MB et al (2022) An experimental investigations on effects of cooling/lubrication conditions in micro milling of additively manufactured Inconel 718. Tribol Int 173:107620. https://doi.org/10.1016/J.TRIBOINT.2022.107620
114. Shabgard M, Seyedzavvar M, Mohammadpourfard M (2017) Experimental investigation into lubrication properties and mechanism of vegetable-based CuO nanofluid in MQL grinding. Int J Adv Manuf Technol 92(9):3807–3823. https://doi.org/10.1007/S00170-017-0319-9
115. Ali ARI, Salam B (2020) A review on nanofluid: preparation, stability, thermophysical properties, heat transfer characteristics and application. SN Appl Sci 2(10):1636-. https://doi.org/10.1007/S42452-020-03427-1
116. Fazeli I, Sarmasti Emami MR, Nazeri MH (2020) Comparing the effect of single and mixture surfactants on the improvement in stability and thermal conductivity of CuO nanofluid: an experimental study. J Therm Anal Calorim 146(2):967–980. https://doi.org/10.1007/S10973-020-10056-8
117. Mishra PC, Mukherjee S, Nayak SK, Panda A (2014) A brief review on viscosity of nanofluids. Int Nano Lett 4(4):109–120. https://doi.org/10.1007/S40089-014-0126-3
118. Singh J, Gill SS, Dogra M, Sharma S, Singh M, Dwivedi SP et al (2022) Effect of Ranque-Hilsch vortex tube cooling to enhance the surface-topography and tool-wear in sustainable turning of Al-5.6Zn-2.5Mg-1.6Cu-0.23Cr-T6 aerospace alloy. Materials. https://doi.org/10.3390/MA15165681
119. Fernando WLR, Karunathilake HP, Gamage JR (2021) Strategies to reduce energy and metalworking fluid consumption for the sustainability of turning operation: a review. Clean Eng Technol 3:100100. https://doi.org/10.1016/J.CLET.2021.100100
120. Gutowski TG, Allwood JM, Herrmann C, Sahni S (2013) A global assessment of manufacturing: Economic development, energy use, carbon emissions, and the potential for energy efficiency and materials recycling. Annu Rev Environ Resour 38:81–106. https://doi.org/10.1146/ANNUREV-ENVIRON-041112-110510/CITE/REFWORKS
121. Karpuschewski B, Kundrák J, Varga G, Deszpoth I, Borysenko D (2018) Determination of specific cutting force components and exponents when applying high feed rates. Procedia CIRP 77:30–33. https://doi.org/10.1016/J.PROCIR.2018.08.199
122. Younas M, Khan M, Jaffery SHI, Khan Z, Khan N (2024) Investigation of tool wear and energy consumption in machining Ti6Al4V alloy with uncoated tools. Int J Adv Manuf Technol 132(7):3785–3799. https://doi.org/10.1007/S00170-024-13548-1
123. Abdelaoui FZE, Jabri A, Barkany AE (2023) Optimization techniques for energy efficiency in machining processes—a review. Int J Adv Manuf Technol 125(7):2967–3001. https://doi.org/10.1007/S00170-023-10927-Y
124. Pawanr S, Gupta K, Pawanr S, Gupta K (2024) Dry machining techniques for sustainability in metal cutting: a review. Processes. https://doi.org/10.3390/PR12020417

125. Khanna N, Rodríguez A, Shah P, Pereira O, Rubio-Mateos A, de Lacalle LNL et al (2022) Comparison of dry and liquid carbon dioxide cutting conditions based on machining performance and life cycle assessment for end milling GFRP. Int J Adv Manuf Technol 122(2):821–833. https://doi.org/10.1007/S00170-022-09843-4
126. Ravi S, Gurusamy P, Mohanavel V (2021) A review and assessment of effect of cutting fluids. Mater Today Proc 37:220–222. https://doi.org/10.1016/J.MATPR.2020.05.054
127. Korkmaz ME, Gupta MK, Çelik E, Ross NS, Günay M (2024) A sustainable cooling/lubrication method focusing on energy consumption and other machining characteristics in high-speed turning of aluminum alloy. Sustain Mater Technol 40:e00919. https://doi.org/10.1016/J.SUSMAT.2024.E00919
128. Ross NS, Manasea Selvin BJA, Nagarajan S, Mashinini PM, Dharmalingam SK, Savio AP, et al. Novel use of cryogenic cooling conditions in improving the machining performance of Al 8011/nano-SiC composites. The International Journal of Advanced Manufacturing Technology 2023; 129:1703–15. https://doi.org/10.1007/S00170-023-12382-1.
129. Balasuadhakar A, Thirumalai Kumaran S, Ahmed F (2023) A review on the role of nanoparticles in MQL machining. Mater Today Proc 72:2828–2832. https://doi.org/10.1016/J.MATPR.2022.07.247
130. Venkatesh R (2025) Synthesis and machining characteristics evaluation of silicon nitride made magnesium alloy composites. SAE Int J Mater Manuf. https://doi.org/10.4271/05-18-03-0017
131. Groover MP. Fundamentals of modern manufacturing : materials, processes, and systems 2010:1012.
132. Bhushan RK (2022) Effect of tool wear on surface roughness in machining of AA7075/ 10 wt.% SiC composite. Compos Part C Open Access. https://doi.org/10.1016/J.JCOMC.2022.100254
133. Mia M, Dhar NR (2016) Optimization of surface roughness and cutting temperature in high-pressure coolant-assisted hard turning using Taguchi method. Int J Adv Manuf Technol 88(1):739–753. https://doi.org/10.1007/S00170-016-8810-2
134. Huang K, Yang W, Chen Q, He S (2015) An experimental investigation of temperature distribution in workpiece machined surface layer in turning. Int J Adv Manuf Technol 85(5):1207–1215. https://doi.org/10.1007/S00170-015-8016-Z
135. Younas M, Jaffery SHI, Khan A, Khan M (2021) Development and analysis of tool wear and energy consumption maps for turning of titanium alloy (Ti6Al4V). J Manuf Process 62:613–622. https://doi.org/10.1016/J.JMAPRO.2020.12.060
136. Zhang X, Yu T, Dai Y, Qu S, Zhao J (2020) Energy consumption considering tool wear and optimization of cutting parameters in micro milling process. Int J Mech Sci 178:105628. https://doi.org/10.1016/J.IJMECSCI.2020.105628
137. Gupta MK, Song Q, Liu Z, Sarikaya M, Mia M, Jamil M et al (2021) Tribological performance based machinability investigations in cryogenic cooling assisted turning of α-β titanium alloy. Tribol Int 160:107032. https://doi.org/10.1016/J.TRIBOINT.2021.107032
138. Jawahir IS, Attia H, Biermann D, Duflou J, Klocke F, Meyer D et al (2016) Cryogenic manufacturing processes. CIRP Ann Manuf Technol 65:713–736. https://doi.org/10.1016/J.CIRP.2016.06.007
139. Wang R, Yang D, Wang W, Wei F, Lu Y, Li Y (2022) Tool wear in nickel-based superalloy machining: an overview. Processes. https://doi.org/10.3390/pr10112380
140. Saraswat M, Sengwa RJ (2023) Effects of PVP surfactant on nanosuspension stability and optical, dielectric, and rheological properties of zinc oxide nanoparticles dispersed alcohols mixture based nanofluids. J Mol Liq 385:122350
141. Ezugwu EO, Wang ZM, Machado AR (1999) The machinability of nickel-based alloys: a review. J Mater Process Technol 86:1–16. https://doi.org/10.1016/S0924-0136(98)00314-8
142. Thakur A, Gangopadhyay S (2016) State-of-the-art in surface integrity in machining of nickel-based super alloys. Int J Mach Tools Manuf 100:25–54
143. Akhtar W, Sun J, Sun P, Chen W, Saleem Z (2014) Tool wear mechanisms in the machining of Nickel based super-alloys: a review. Front Mech Eng 9(2):106–119. https://doi.org/10.1007/s11465-014-0301-2
144. Denkena B, Biermann D (2014) Cutting edge geometries. CIRP Ann 63:631–653
145. Liang J, Gao H, Xiang S, Chen L, You Z, Lei Y (2022) Research on tool wear morphology and mechanism during turning nickel-based alloy GH4169 with PVD-TiAlN coated carbide tool. Wear 508:204468
146. Kulkarni P, Chinchanikar S (2022) A review on machining of nickel-based superalloys using nanofluids under minimum quantity lubrication (NFMQL). Journal of The Institution of Engineers (India): Series C 104(1):183–199. https://doi.org/10.1007/s40032-022-00905-w
147. Kumar G, Sen B, Ghosh S, Rao PV (2024) Strategic enhancement of machinability in nickel-based superalloy using eco-benign hybrid nano-MQL approach. J Manuf Process 127:457–476. https://doi.org/10.1016/j.jmapro.2024.08.015
148. Alves SM, Mello VS, Faria EA, Camargo APP (2016) Nanolubricants developed from tiny CuO nanoparticles. Tribol Int 100:263–271

Publisher's Note Springer Nature remains neutral with regard to jurisdictional claims in published maps and institutional affiliations.

Springer Nature or its licensor (e.g. a society or other partner) holds exclusive rights to this article under a publishing agreement with the author(s) or other rightsholder(s); author self-archiving of the accepted manuscript version of this article is solely governed by the terms of such publishing agreement and applicable law.